AN ABSTRACT OF THE THESIS OF

Jeff Phillippe for the degree of Master of Science in Water Resource Science presented on June 6, 2008.

Title: Present-day and Future Contributions of Glacier Melt to the Upper Middle Fork Hood River: Implications for Water Management

Abstract approved: _____

Anne W. Nolin

Glaciers are effective reservoirs because they moderate variations in runoff and supply reliable flow during drought periods. Thus, there needs to be a clear understanding of the influence of glacier runoff at both the basin and catchment scale. The objectives of this study were to quantify the late summer contributions of glacier melt to the Upper Middle Fork Hood River and to simulate potential impacts of climate change on late summer streamflow. The Upper Middle Fork Hood River catchment (50.6 km^2) is located on the northeast flanks of Mount Hood Oregon. Discharge measurements and isotope samples were used to calculate glacier meltwater contributions to the entire catchment, which feeds into a major water diversion used for farmland irrigation. Data were collected over the period August 10 – September 7, 2007. This late summer period was selected because there is typically little rain and suspected high glacier melt contributions. Discharge measurements taken at glacier termini, show that just two of the mountains glaciers, Eliot and Coe, contributed 41% of the total surface water in the catchment. The Eliot Glacier contributed 87% of the total flow in the Eliot Creek, while the Coe Glacier supplied 31% of the runoff in Coe Creek. Isotopic analyses, which include the inputs of all other glacier surfaces in the

catchment, show a total glacier contribution of 88% from the Eliot Glacier to the Eliot Creek, in excellent agreement with the streamflow measurements. Isotopes also showed an 88% contribution from the Coe Glacier to the Coe Creek, higher than the amount measured from streamflow. This latter discrepancy is likely due to undersampling of streamflow from the Coe Glacier. During the isotope measurement period, overall contributions of both Coe and Eliot Glaciers to the Upper Middle Fork Hood River were 62 – 74% of catchment discharge. A temperature index model was used to simulate projected impacts of glacier recession and warmer temperatures on streamflow. The Snowmelt Runoff Model (SRM) was chosen for this task because it has been shown to effectively model runoff in glacierized catchments where there are limited meteorological records. SRM was calibrated using the 2007 discharge records to quantify August – September glacier runoff in the Upper Middle Fork catchment under a variety of glacier and temperature scenarios. SRM simulations indicate that runoff from the catchment glaciers are highly sensitive to changes in glacial area, glacier debris-cover, and air temperature. Model simulations show that glacier recession has a greater effect on runoff than do projected temperature increases. Thus, even without warmer summer temperatures, glacier contributions to streamflow will decrease as long as the glacier continues to lose mass. Applying both current glacier recession rates and a 2°C temperature forcing, the model predicts a decrease of 31% of late summer glacier runoff by 2059, most of which is lost in August. This study suggests that glaciers currently play a significant hydrological role in the headwater catchments of the Hood River Basin at a time when water is needed most, and that these contributions are projected to diminish over time.

Present-day and Future Contributions of Glacier Melt to the Upper Middle Fork Hood River: Implications for Water Management

by

Jeff Phillippe

A THESIS

submitted to

Oregon State University

in partial fulfillment of

the requirements for the

degree of

Master of Science

Presented June 6, 2008

Commencement June 2009

Master of Science thesis of Jeff Phillippe presented on June 6, 2008.

APPROVED:

_____

Major Professor, representing Water Resource Science

_____

Director of the Water Resources Graduate Program

_____

Dean of the Graduate School

I understand that my thesis will become part of the permanent collection of Oregon State University libraries. My signature below authorizes release of my thesis to any reader upon request.

_____

Jeff Phillippe, Author

ACKNOWLEDGEMENTS

First and foremost, I would like to thank my advisor Anne Nolin, who introduced me to the Water Resources Graduate Program, and was instrumental in the development of this thesis. I am grateful to my committee members, Jeff Shaman, Gordon Grant, and Jill Davidson, who all contributed constructive revisions during the completion of the project. Anne Jefferson and Sarah Lewis were also part of this project from the beginning and I thank them for their input and for helping me to set up my stage recorders. Volunteer field assistants David Elwood and Robert Denner were of particular help in sample collections, and Jiayin Lai was a great field partner, as she shared much of the driving to field sites and assisted in late-night discharge measurements. I am grateful to a long list of faculty in the Geosciences Department and the Water Resources Graduate Program, who were always willing to meet and provide constructive feedback during the course of the project. I was fortunate to work with the Middle Fork Irrigation District office, who assisted my field work and gave me road access to many of my sites throughout the summer. Finally, I would like to thank all of the organizations which provided grants to make this thesis happen: The Institute for Water and Watersheds at Oregon State University, the Geological Society of America, the Mazamas, and the American Association of Geographers Mountain Specialty Group.

TABLE OF CONTENTS

Page

TABLE OF CONTENTS (Continued)

LIST OF FIGURES

LIST OF FIGURES (Continued)

LIST OF TABLES

LIST OF APPENDICES

Chapter 1: Introduction

With glaciers disappearing at record rates, there needs to be a clear understanding of the influence of specific glaciers on basin discharge. On a global scale, alpine glaciers have been receding since the Little Ice Age, and the continuation of warming trends will further accelerate this retreat in the foreseeable future (IPCC 2007a). This glacial net mass loss will inevitably affect both the timing and volume of streamflow. Furthermore, as glaciers shrink basins will become more reliant on snowmelt, and peak runoff will occur earlier in the melt season.

The effect of glacier retreat on water resources is a major concern for basins that experience late-summer low flows because glaciers contribute to runoff later in the melt season than do snow-covered basins. Glaciers impart delays in summer peak streamflow for two reasons: 1) they supply a seasonally inexhaustible supply of meltwater that will peak in response to temperature maxima, and 2) there is a lag effect caused by glacial storage and the delayed networking of englacial and subglacial conduits (Jansson et al., 2003). Glaciers also provide a dependable water supply in years of drought, whereas areas that are traditionally snow-covered will not (Fountain and Tangborn 1985). Krimmel and Tangborn (1974) show that in the Pacific Northwest, interannual runoff variation is minimized in basins with 30% glaciation; basins at less than 10%, on the other hand, are prone to severe variation, especially during the months of July and August (Fountain and Tangborn 1985).

Glaciers on Mount Hood, Oregon have receded up to 61% of their length in the last century (Lillquist and Walker, 2006). However no study has modeled the impact of Hood's glaciers on downstream flow, nor are there any historical discharge data within

its alpine catchments. This study investigates the contribution of glacier melt specifically to the Upper Middle Fork Hood River catchment (50.6 km^2) on the northeast flanks of Mount Hood Oregon, because it has a relatively large glacierized area (6.6%) and is directly above the Middle Fork Irrigation District (MFID) diversion system. The first objective of this study is to combine discharge measurements, diurnal runoff characteristics of glaciers, and a stable isotope analysis to measure the glacier meltwater contribution to the Upper Middle Fork Hood River in the late summer of 2007. The second objective is to model glacier runoff under future glacier recession and climate change scenarios.

1.1 Glacier Melt and Runoff Processes

The hydrological properties of glacierized basins differ from glacier-free basins in a variety of ways. It is estimated that glaciers in the U.S.A. release 2-10 times more water than do neighboring catchments of equal area and altitudes (Mayo, 1984). Furthermore glacierized catchment runoff is controlled primarily by energy fluxes whereas glacier-free catchments are dominated by precipitation patterns (Jansson et al., 2002). Braun et al. (2000) found that glacierized catchments in the Alps are more sensitive to global warming than are the mountainous watersheds of Bavaria, which are mostly glacier-free. Finally, for reasons described later in this section, glacier discharge peaks much later in the melt season than does snowmelt runoff (Singh and Singh, 2001).

The unique characteristics of glacierized catchments are due to the complicated passage of meltwater through a glacier. Early in the melt season, ablation zone

meltwater must percolate through the snowpack before it can discharge down-glacier. As the snowpack thins over the course of the ablation season, the residence time of meltwater decreases, and runoff peaks earlier in the day. As the ice surface becomes exposed, runoff becomes more immediate and there is a more pronounced diurnal response in proglacial streams (Fountain and Walder, 1996). This runoff will either travel on the surface of the glacier ice momentarily or in seasonal supraglacial streams (Figure 1.1). The meltwater then falls through a moulin or crevasse which allow for immediate access to englacier networks and subglacial flow.

Figure 1.1 Supraglacial stream on the Eliot Glacier ablation zone (left) and a moulin in the Coe Glacier ablation zone.

Meltwater in the accumulation zone must percolate through the snowpack and then through a firn layer. The firn layer also delays runoff because as water percolates through unsaturated firn, it encounters near-impermeable glacier ice and backs up to fill 40% of the firn pores (Schneider, 2000; Fountain, 1989). Water is not released until the

firn ripens and its capillary deficit is met (Jansson et al., 2003). Firn also serves to attenuate diurnal variations in runoff later in the ablation season, and is the likely source of baseflow in proglacial streams (Fountain, 1996). Golubev (1973) proposes that the lag time of the firn area is about ten times longer than that of the ablation zone.

Englacial conduits exist in the accumulation areas and more extensively in the ablation zones, and serve as a connection between surface drainage and subglacier conduits. Englacial pathways can be quite long and in most cases converge with the glacier bed in the ablation zone (Fountain and Walder, 1998). The conduits which originate from the accumulation area regulate their diameters so that the channel is always full of water and is constantly pressurized. Ablation zone conduits, however only maintain high pressure during peak melting or precipitation events (Fountain and Walder, 1998). The englacial channels converge with subglacial conduits, which are carved at the ice/bedrock interface. A subglacial arborescent drainage system may exist, but normally converges to one outlet at the glacier terminus. The development and connection of this network is usually completed mid-way through the ablation season (Singh and Singh, 2001), and is largely responsible for the lagged timing of glacier runoff.

1.2 Stable Isotope Studies in Mountain Catchments

Hydrologic studies in mountainous areas have extensively used stable isotopes in a variety of applications. Dincer et al. (1970) first used isotopes in the hydrograph separation of a Czechoslovakian catchment to show that 63% of surface water was derived from the subsurface and ground. Sklash and Farvolden (1979) made famous the use of Oxygen-18 tracers when they showed the dominance of pre-event water in storm hydrographs. Several snowmelt studies (Rhode, 1981; Obradovic and Sklash, 1986) have used ^{18}O and Deuterium concentrations to confirm that also during snowmelt events, groundwater comprises the bulk of the hydrograph. Earman et al. (2006) used stable isotope techniques to deduce that snowmelt contributes at least 40-75% of the groundwater recharge in areas of the Southwestern United States, while only 25-50% of the annual precipitation in these areas fall as snow. This study also reports that there is a significant difference in the stable isotopic composition of the snowpack and the meltwater that is released from that snowpack. Furthermore past studies have shown that during snowmelt events, the initial meltwater is isotopically lighter than the average conditions of the snowpack but becomes more enriched in ^{18}O through time (Rodhe, 1981; Shanley et al., 1995). It has been recently confirmed (He et al., 2001; Stichler and Schotterer, 2000) that stable isotopes in glaciers, like those in snow, are sensitive to changes in elevation, temperature, and evaporation, and that variation in the isotopic composition of glacier meltwater is to be expected.

Mountain glacier studies have used ^{18}O distributions in extracted ice cores to account for historical climates (Thompson et al., 1981) and more recently in the analysis of glacier meltwater contributions at the basin-scale (Mark and Selzer, 2003).

The later study incorporated discharge measurements, hydrochemical samples, and an end-member mixing model of oxygen isotopes to project a glacier meltwater contribution of 30-45% of the total annual discharge for catchments in the Cordillera Blanca, Peru. There is little research however which incorporates isotopes in the derivation of glacier meltwater at the catchment scale in the mid-latitudes.

1.3 Glacier Melt Models

In the last three decades there have been several approaches to modeling glacier melt in alpine areas, beginning with simple empirical relationships and progressing to data-intensive physically-based models (Lundquist, 1982.; Escher-Velter, 1985; Martinec and Rango, 1986; Willis et al., 2002). Glacier melt modeling is typically of two forms: temperature-index and energy balance (Hock, 2005). Temperature-index models are based on the relationship between temperature and ice/snowmelt, and are more prevalent worldwide because they rely on few meteorological variables (Rango and Martinec, 1995).

Energy balance models on the other hand are data-intensive, and are limited to areas where wind speed, relative humidity, temperature, long-wave radiation, and short-wave radiation are measured or can be appropriately estimated. Energy balance inputs have been applied to snow and glacier surfaces in the following form:

$$\Delta Q = S_{net} + H + L_v E + G + M \qquad (1.1)$$

where ΔQ is the snowpack energy, and S_{net}, H, L_vE, G, and M are the total radiative, sensible, latent, conductive, and advective energy fluxes (Escher-Velter, 1980; Male and Granger, 1981; Marks and Dozier, 1992).

Both model types have been integrated into glacier runoff models, which are often modified from pre-existing snowmelt runoff models (Singh and Singh, 2001). Glacier runoff models can be divided into two processes: the onset of icemelt and the progression of that meltwater out of the glacier. The former process is better understood and more accurately calculated (Fountain and Tangborn, 1985), but recent models are beginning to capture the variability in runoff processes.

1.4 Previous Applications of Glacier Runoff Models

Anderson (1973) proposed a snowmelt model that would later be modified to predict glacier runoff. He combined a simple temperature-index approach during the dry season with a mass balance approach (similar to Equation 1.1) during rainy periods to generate meltwater. His temperature index calculation required the multiplication of an empirically derived melt factor. The model was modified to represent glaciers as areas with snow depths large enough to prevent complete melt-out over the course of the water year. The minimum snow-covered area (SCA) at the end of the ablation season, which was generated according to depletion curves derived from basin snow-water equivalent (SWE), was delineated as glacier area. The model proved to be an effective long-term predictor of glacier melt, but often generated flow too quickly out of the glacier and was deemed less effective at the daily time-step (Fountain and Tangborn, 1985).

Quick and Pipes (1977) designed the more sophisticated University of British Columbia Watershed Model (UBC), which requires temperature, precipitation, empirically-derived temperature and precipitation lapse rates, surface permeability, and basin SWE as inputs into the calculation of glacier melt. The model uses user-specified elevation bands to spatially distribute melt throughout the basin. The model allows for either a temperature-index or an energy balance calculation, the later of which can be estimated when only temperature data is available. Power and Young (1979) modified the temperature-index based UBC Watershed Model to include a glacier computation. They specified glacier zones, which supply meltwater even when that year's snowpack is completely diminished. The model underestimated peak flows, particularly in the late melt season, probably because it does not accurately represent the storage and drainage of meltwater through a glacier (Singh and Singh, 2001).

Escher and Velter (1980) developed the physically-based Escher-Velter (EV) model, which can determine glacier melt at any location on a glacier at 1-hour time-steps. The model incorporates air temperature, relative humidity, precipitation, and wind speed and divides the basin into three surface zones: snow, firn, and ice. A storage term (k) is derived for each zone so that the timing of runoff can be better represented than has been in the aforementioned studies. Runoff is derived from a combination of meltwater in these three zones and a constant groundwater input. In-situ solar radiation measurements quantify and spatially distribute radiation reception and albedo for the entire glacier surface. A comparison of model results with measured runoff (Baker et al., 1982) on the Vernagtferner Glacier (Austria), shows good temporal

resolution, but accuracy may be compromised because runoff is not included from non-glaciated sections of the basin (Singh and Singh, 2001).

In the last decade, several snow and glacier melt studies have incorporated energy fluxes into temperature-index models. This method is appropriate for areas that have limited data but could use better estimations of sub-daily variations in runoff, which are often misrepresented in temperature-index models (Hock, 2003). Kustas et al. (1994) combined a simplified radiation budget with a degree-day model and found simulation runs to be equally accurate to those using the energy balance approach. Brubaker et al. (1996) used this same approach at the W-3 research basin in Vermont, USA and found a better fit for two of their six validation tests when the radiation version was used instead of the simple degree-day version.

Recent studies have modified the Distributed Hydrology Soils Vegetation Model (DHSVM) to measure glacier melt contributions in basins in the North Cascades, Washington (Chennault, 2006; Donnell, 2007). DHSVM, developed by Wigmosta et al. (1994) is a physically-based spatially-distributed model that is data intensive. It incorporates all of the variables necessary to the energy balance equation (1.1) as well as distributed basin parameters, including elevation, aspect, slope, vegetation cover, soil type, and soil thickness. Chennault (2004) incorporated glacier area into the vegetation cover parameter, and set it as inexhaustible snow layer. His simulations show that glaciers contribute 0.6% to 56.6% of the annual flow in the Thunder Creek Watershed, Washington and that forecasted glacial retreat could reduce annual discharge by more than 30% in the next 100 years.

1.4 The Snowmelt Runoff Model

This study uses SRM instead of an energy balance model because the uncertainty in its application is likely smaller than the uncertainty involved in the extrapolation of remote meteorological data and the subsequent estimation of energy fluxes. Furthermore, SRM has obtained excellent results in high altitude terrain (Ferguson, 1999) and has recently been validated for use in glacier melt computations (Schaper and Seidel, 2000). Using a temperature-index model like SRM is often justified because the meteorological data necessary to compute energy fluxes are frequently unavailable. However, recent research (Ohmura, 2001; Kuhn, 1993) suggests that there is also a physical justification for using air temperature as an index for calculating melt. The primary heat sources for melt, radiation and sensible heat flux, are highly correlated with temperature. Additionally, the energy balance input that is least correlated with temperature, wind speed, is a very small contributor to melt (Ohmura, 2001).

SRM was first developed by Martinec (1975) to model snowmelt runoff in high European catchments and has since become a widely-used tool for forecasting runoff in snow-dominated basins around the world (WMO, 1986). The most recent version WinSRM 1.11 is currently available online in a Windows™ environment. SRM is considered semi-distributed because it spatially distributes parameters according to specified elevation zones. The input parameters and variables necessary to initiate SRM are provided in Table 1.1.

Table 1.1 Standard Inputs in the Snowmelt Runoff Model. All of the parameters and variables can be changed temporally and for each elevation zone.

Basin Characteristics	Parameters	Variables
Basin and Zone Areas	Degree Day Factor	Temperature
Area Elevation Curve	Runoff Coefficient	Precipitation
(DEM)	Temperature Lapse Rate	Snow-Covered Area
	Rainfall Contributing Area	Initial Runoff
	Recession Coefficient	Recession Coefficient
	Time Lag	

SRM uses a degree-day method to calculate total ice and snowmelt. This method determines the decrease in SWE from a snowpack by subtracting base temperature (usually 0°C) from the daily air temperature and multiplying by a coefficient (the degree-day factor):

$$M = a\,(T_a - T_b) \qquad (1.2)$$

where a is the degree-day factor (cm $°C^{-1}$ d^{-1}), T_a is the mean daily temperature (°C), T_b is the base temperature (°C), and M is the snowmelt rate (cm d^{-1}) (Kustas et al., 1994). The degree-day factor (DDF) is typically measured empirically with snow lysimeters or ablation stakes, but can also be estimated according to the density of the snowpack (Martinec, 1960).

To model the actual runoff of glacier meltwater SRM requires recession and runoff coefficients, both of which can be derived from historical hydrographs. The final computation of runoff in SRM takes the following form:

$$Q_{n+1} = [c_{Sn} \cdot a_n (T_n + \Delta T_n) S_n + c_{Rn} P_n] \frac{A \cdot 10000}{86400} (1\text{-}k_{n+1}) + Q_n k_{n+1} \quad (1.3)$$

where: Q = average daily discharge [$m^3 s^{-1}$]

c = runoff coefficient expressing the losses as a ratio (runoff/precipitation), with c_S referring to snowmelt and c_{Rn} to rain

a = degree-day factor [cm $^oC^{-1}$ d^{-1}] indicating the snowmelt depth resulting from 1 degree-day

T = number of degree-days [^oC d]

ΔT = the adjustment by temperature lapse rate when extrapolating the temperature from the station to the average hypsometric elevation of the basin or zone [^oC d]

S = ratio of the snow covered area to the total area

P = precipitation contributing to runoff [cm].

A = area of the basin or zone [km^2]

-Martinec and Rango (2007)

1.6 Study Site Description

Located on the north side of Mount Hood, Oregon (Figure 1.2), the Middle Fork drains into the Hood River, which flows into the Columbia River, and eventually into the Pacific Ocean. The Hood River discharges in response to a highly seasonal pattern of precipitation and snowmelt events. The Aleutian Low contributes to high precipitation during the winter months, whereas the arrival of the North Pacific High gives way to dry summers (Walters and Meier, 1989). Runoff is high in the winter months when there are high rates of rainfall in the lower elevations of the basin. It remains high throughout the spring as the snowy slopes of Mount Hood and adjacent mountains melt off. The summer and early fall however, experience severe low flows in response to minimal precipitation inputs and the disappearance of the seasonal snowpack (Figure 1.3).

Figure 1.2 Location map for the Hood River Basin, OR. DEM data source - USGS EROS Data Center

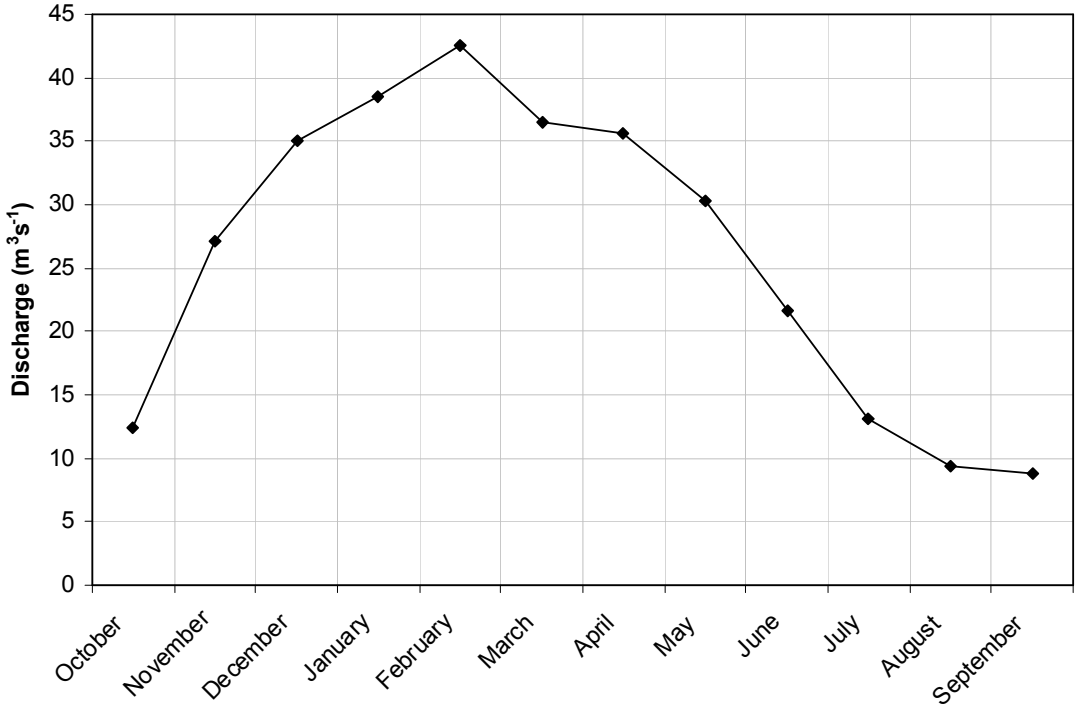

Figure 1.3 30-year monthly average discharge of Hood River. Stage was recorded at the USGS gauging site (#14120000) at Tucker Bridge.

1.61 *The Hood River Basin*

The Hood River Basin is 882 km^2 and encompasses the towns of Parkdale, Odell, Dee, and Hood River (Figure 1.4). The basin relies first on agriculture, followed by lumber, and tourism as its prime sources of revenue and industry. The Hood River irrigates more than 5300 ha of commercial pear, apple, and peach orchards, and the Hood River County leads the world in the production of Anjou pears (Hood River County, 2003). The watershed contains approximately 650 km of perennial streams, of which 150 km are spawning grounds for anadromous fish (Hood River Local Advisory Committee, 2004).

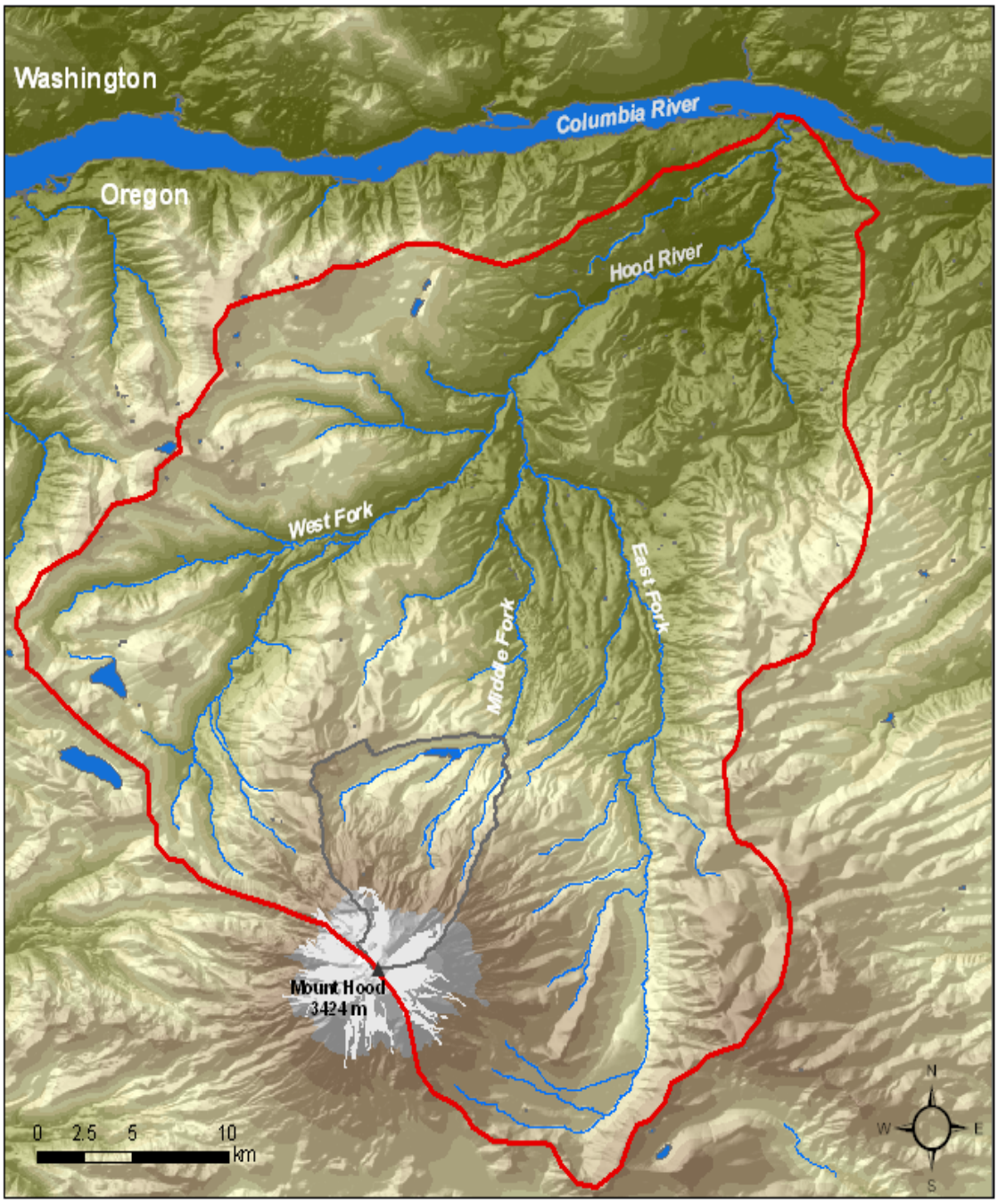

Figure 1.4 The Hood River Basin (red) and the Upper Middle Fork Catchment (grey). DEM source – USGS National Elevation Dataset

1.62 *The Upper Middle Fork Catchment of the Hood River*

Because it has a relatively high fraction of glacier area (6.6%) and is upstream of any diversions, the Upper Middle Fork catchment (50.6 km^2) of the Hood River was selected as the study area for investigations in this paper. The catchment consists of 4 creeks that drain the north side of Mount Hood: Eliot, Coe, Clear and Pinnacle (Table 1.2; Figure 1.5). Eliot and Coe are glacier-fed, whereas Clear and Pinnacle rely solely on lingering snowpacks and groundwater inputs during the summer dry season. The tree line ranges from 1970 to 2300 m and alpine vegetation is sparse. Forests within the catchment consist of Pacific silver fir, mountain hemlock, whitebark pine, lodgepole pine, Douglas fir, western red cedar, western hemlock, western larch, western white pine, ponderosa pine, and Oregon Oak (Lundstrom, 1992).

Clear and Pinnacle Creeks flow into Laurance Lake Reservoir, which acts as a storage and a power supply for the Middle Fork Irrigation District (MFID). Because the Eliot is more sediment-laden, it is diverted directly from the channel to a settling pond, and after sufficient deposition of clays and silts, the water is pumped out by the irrigation district. The Coe Creek is also sediment-laden, but without a settling pond, its diversion system is intermittently shut down during times of high turbidity. The MFID distributes this water to 421 customers in the Parkdale area, for irrigation of 2574 of the 3398 hectares in the region. Extraction from these mountain creeks become especially important in the late summer as this is the harvest period for apples and pears (pers. communication – Dave Compton and Craig DeHart, MFID, 6/2/08).

Table 1.2 Spatial Properties of the Upper Middle Fork Hood River tributary creeks.

Creek	Catchment Area (km^2)	Creek Length (km)	Glacier Fraction (%)	Elevation Range (m)
Eliot	9.6	8.3	18.9	821-3424
Coe	17.5	8.0	8.7	833-3271
Clear	14.9	7.2	0	892-2132
Pinnacle	7.0	5.4	0	892-1853
Total Catchment	50.6	28.9	6.6	821-3424

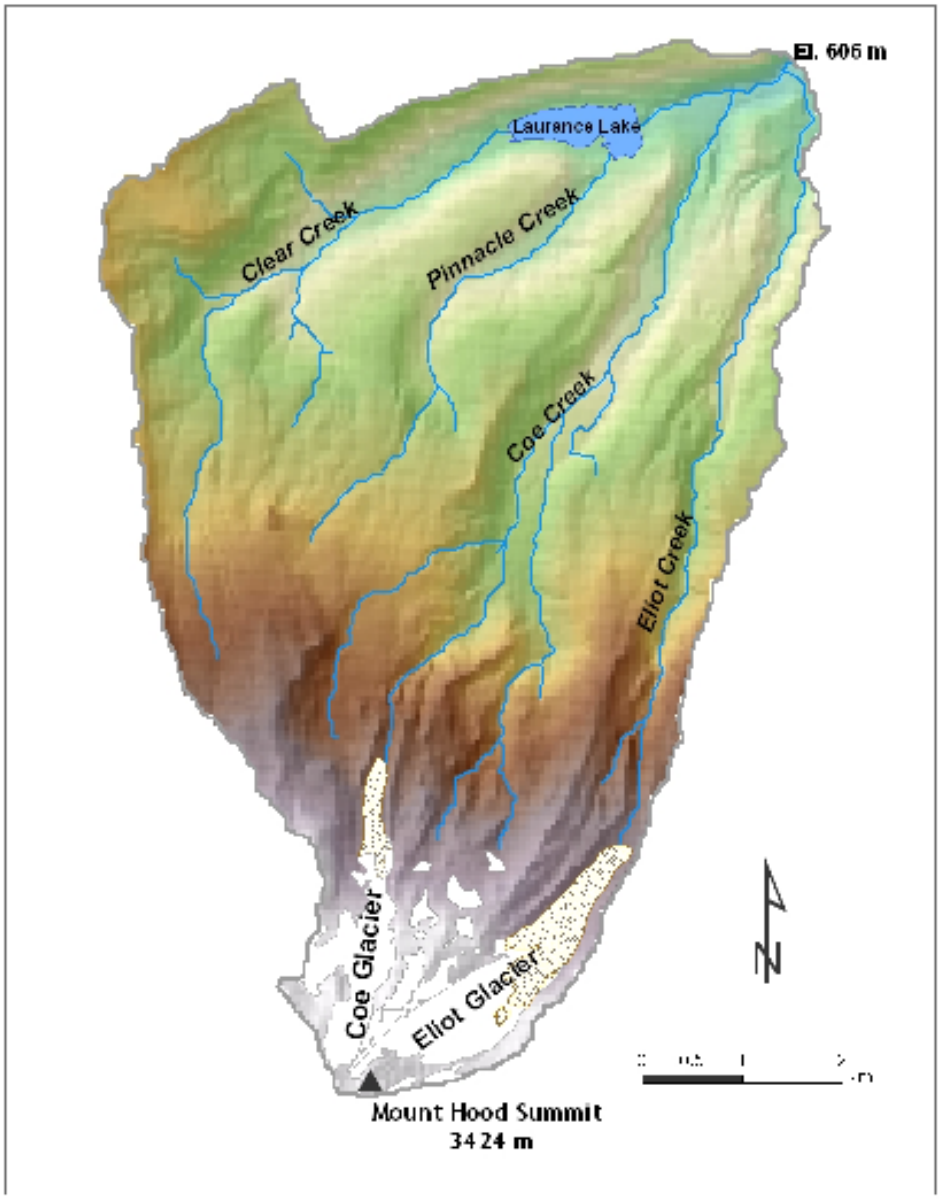

Figure 1.5 Surface flow inputs to the Upper Middle Fork Hood River.

1.63 *Mount Hood*

Mount Hood (3424 m) is the highest mountain in Oregon and covers an area of 200 km^2 and a volume of 50 km^3 (Sherrod and Smith, 1990). The mountain stands as a major orographic obstruction to the eastward flow of moist Pacific air masses, and like the rest of the Cascade Range, divides the state between the wet west side and the drier east side. A stratovolcano, Mount Hood developed during the middle and late Quaternary Period (since 0.73 Ma BP) as a combination of lava flows and pyroclastic deposits (Lundstrom, 1992), and it is estimated that andesitic flows make up 70% of the total mountain material (Wise, 1968). The most recent major eruptions date back to 1760 and 1810, and produced pyroclastic flows and massive lahars which travelled up to 80 km (Cameron and Pringle, 1987).

Mount Hood is host to 11 major glaciers, which total 13 km^2 in area and 0.4 km^3 in volume (Lillquist and Walker, 2006). Between 1907 and 2004, Mount Hood glaciers (Figure 1.6) receded by an average of 38% in area. Located in the Upper Middle Fork catchment, the Coe (1.26 km^2) and Eliot Glaciers (1.61 km^2) have receded at rates significantly slower than those of neighboring glaciers, with area losses of 15 and 19% respectively (Jackson, 2007). Their slower rates of recession may be explained by significant debris cover in their ablation zones, their northerly aspects, and relatively high altitudes. These glaciers are assumed to have significant contributions to the Middle Fork (Millstein, 2006), but there are few records which quantify their runoff.

Figure 1.6 2007 photos of the Eliot (top) and Coe (bottom) glaciers. On the left side of the Coe photo are remnant glacierettes of the Langille Glacier.

Chapter 2: Field Methods

2.1 Measurement of Runoff

Stream discharge was measured from June to September, 2007 immediately upstream of the diversions of the four catchment creeks: Eliot, Coe, Pinnacle, and Clear. Runoff at the outlet of Coe and Eliot Glaciers was also measured between August and September, 2007 to determine the contribution of flow from the glaciers to the downstream sites (figure 2.1). Automated measurements of water height were recorded using Odyssey™ capacitance water height recorders. A 15-minute time step was used at each of the six sites (Figure 2.2). Three of the six sites lacked trees for mounting the recorders. In these areas, a rock hammer drill was used to install metal extensions between riparian boulders and the recorders. At each of the six sites, 6 - 14 stream discharge measurements were computed by measuring flow velocity and water depth along a transect across the stream. Flow velocity was measured using a Marsh-McBirney™ velocity meter and water depth was measured using a "Jacob's staff". These discharge measurements were then used to develop a rating curve that was used to convert values of water height (from the automated capacitance sensors) to stream discharge.

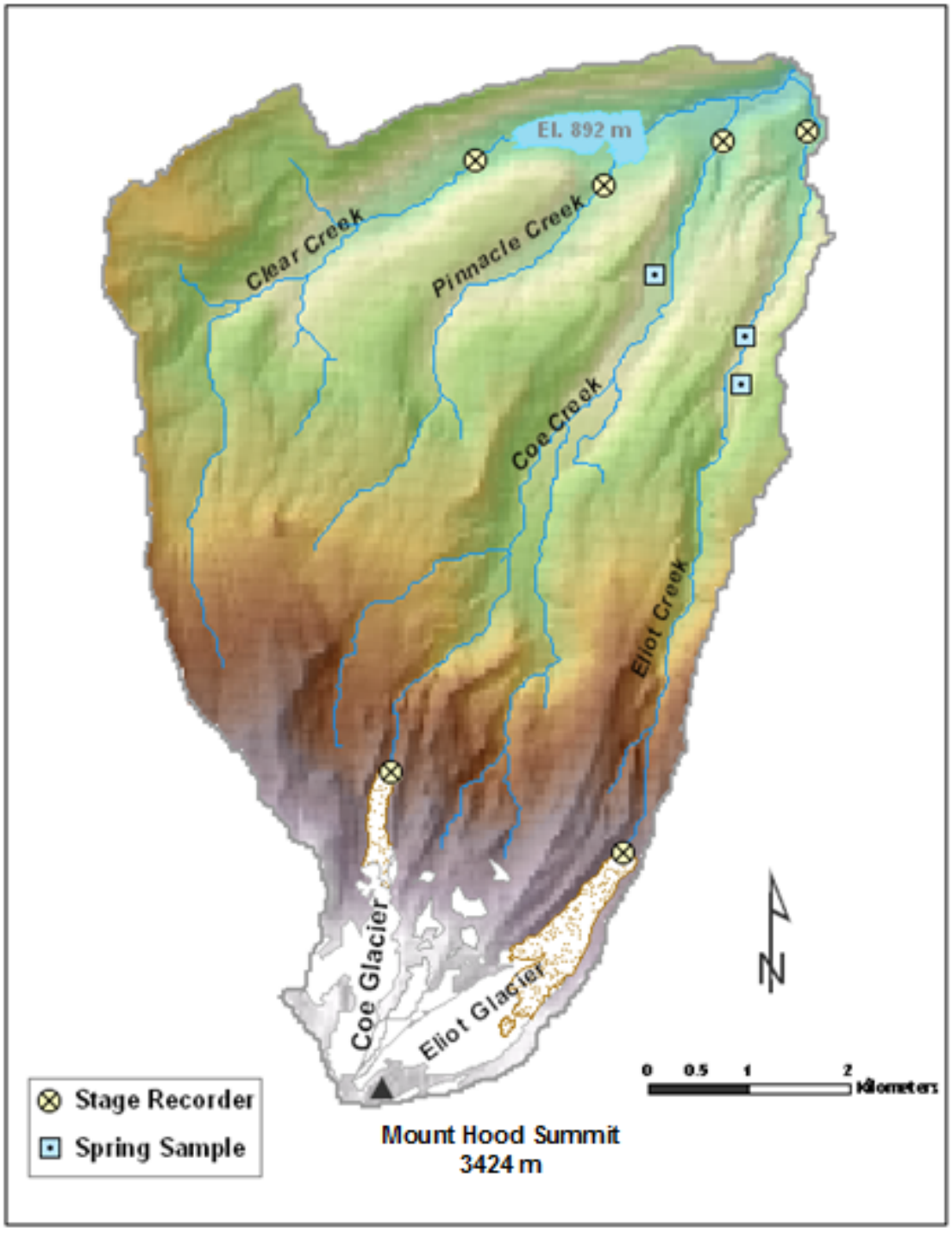

Figure 2.1 Location of water height recorders and spring samples in the Upper Middle Fork catchment.

Figure 2.2 Water height recorders located at Eliot Creek (a), Eliot Creek Culvert (b), Eliot Glacier (c), and Coe Glacier (d). Sediment buildup at site a. necessitated the new site b. midway through the field season.

Due to the debris flow event of November, 2006 there was a large amount of loose sediment within the Eliot and Coe channels and additional unconsolidated material along the banks. Aggradation rates were high in stagnant sections of the creek, particularly in the eddy where the first Eliot recorder was installed. Three weeks after its installation, more than 50 cm of sediment buried its base. It was thus necessary to reposition the instrument to a more dynamic section of the creek in an area less prone to deposition (Figure 2.2). Sediment build-up in the three other sites on Eliot and Coe was less severe, but occasionally required clearing at the bed. To compensate for the changes in local stream height caused by deposition, the rate of aggradation between measurements was calculated, assumed constant, and was subtracted from each height recording over time.

After downloading the height data at the end of the field season, rating curves generated exponential relationships between water height and discharge (Appendix A). This enabled the interpolation of discharge at the 15-minute time step for the entire study period.

2.2 Stable Isotope Analysis

Water samples were collected on three occasions throughout the basin in August, September, and October (Figure 2.1) for the analysis. 60 ml high-density polyethylene bottles were capped underwater and the caps were taped to keep bottles air-tight. Stream surveys located only three lateral streams within the Coe and Eliot catchments, each of which were fed by springs within 40 m of the mainstem. Their mean ^{18}O composition served to quantify non-melt contributions. To characterize glacier melt, samples were collected 5 m downstream of the Eliot and Coe Glacier

termini. Samples were analyzed for $\delta^{18}O$ at the Isotope Ratio Mass Spectrometer Facility at Oregon State University (Corvallis, OR). They were run through a Finnigan™/MAT 252 (dual inlet) and were reported relative to SMOW (Standard Mean Ocean Water; Craig, 1961) with a precision of +/-0.03 permil.

Modifying the standard equations for a two-component mixing model (Sklash and Farvolden, 1979) glacier meltwater replaced new water in order to solve for the relative proportions of groundwater (old water) and glacier melt:

$$Q_{stream} = Q_{old} + Q_{glaciermelt} \quad (2.1)$$

$$\mathcal{P}_{old} = \frac{Q_{old}}{Q_{stream}} = \frac{C_{stream} - C_{glaciermelt}}{C_{old} - C_{glaciermelt}} \quad (2.2)$$

$$\mathcal{P}_{glaciermelt} = \frac{Q_{glaciermelt}}{Q_{stream}} = \frac{C_{stream} - C_{old}}{C_{glaciermelt} - C_{old}} \quad (2.3)$$

where Q is discharge, $\mathcal{P}$ is the proportion of the indicated component, and C is the isotopic composition. To compare meltwater composition with glacier ice, four Eliot ice samples were collected between 2000 and 2300 meters in elevation. Using an ice axe, the surface ice was cleared and samples were collected at depths of at least 4 cm.

Chapter 3: Snowmelt Runoff Model Inputs

3.1 Input Variables

3.11 *Temperature and Precipitation*

Daily maximum and minimum temperature values were used as an input into the calibration of SRM., and was acquired from the Mount Hood Meadows-Base Weather Station (station ID# MHM52; Table 3.1), accessible from the Mesowest Database (http://www.met.utah.edu/mesowest). Only five maximum/minimum values from the August-September period were missing and were calculated by linearly interpolating temperatures from the previous day.

Table 3.1 Meteorological stations consulted in the SRM calibration and runoff simulations. The Red Hill SNOTEL site was solely used in generating a precipitation lapse rate.

Name	Station ID	Altitude (m)	Coordinates	Period of Data Extraction
Mount Hood SNOTEL	21D08S	1637	45.32°N, 121.71°W	1981-2007 (Aug./Sept.)
Red Hill SNOTEL	21D04S	1341	45.47°N, 121.70°W	1998-2007 (Aug./Sept.)
Mount Hood Meadows - Base	MHM52	1600	45.33°N, 121.6°W	2007 (Aug./Sept.)

Precipitation data was taken from the Mount Hood Snow Telemetry (SNOTEL) site (Table 3.1). Precipitation during the August-September study period was expectedly minimal, and there were only two short events, amounting to less than 4 cm of rain. 25-year mean daily temperature data and 27-year mean daily precipitation data from the available record from the Mount Hood SNOTEL site served as the standard meteorological inputs into all of the SRM simulations.

3.12 *Glacier-Covered Area*

In this study, glacier-covered area (GCA) takes the place of the standard snow-covered (SCA) area in SRM, and is a parameter that can be determined using satellite remote sensing. Because of its availability in the Mount Hood region at end of the water year, and its appropriate spatial resolution (15-90 m), September 10, 2006 ASTER (Advanced Spaceborne Thermal Emission and Reflection Radiometer) images (Figure 3.1) were used to delineate Eliot and Coe glaciers as well as the glacierettes and snowfields of the Compass Catchment. Since glaciers exhibit only small changes in areal extent during one ablation season, the GCA was assumed to be constant throughout the two-month study period.

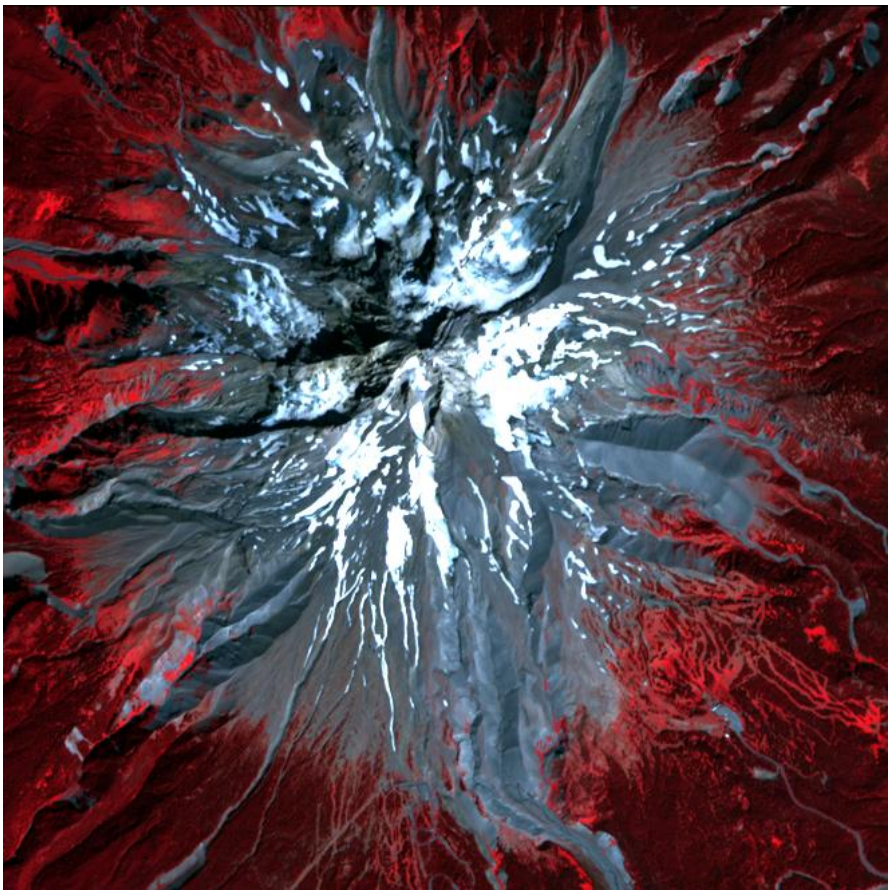

Figure 3.1 False color image of Mount Hood from ASTER, Sept. 10, 2006

ASTER provides 14 bands of data, from the visible to the thermal-infrared wavelengths. Utilizing a zoom lens on the satellite Terra, ASTER can also provide high resolution digital elevation models (NASA, 2004), which were utilized in this study. Because radiance is accurately measured for only cloud-free pixels, ASTER provides a "cloud mask" to indicate which pixels should be avoided in data analysis (NASA, 2004).

The calculation of glacier coverage has traditionally used the ratio of ASTER bands 3 and 4 (Taschner and Ranzi, 2002). These bands were used for the upper debris-free portions of Coe and Eliot Glaciers, but do not suffice for the lower sections covered in debris. Instead National Agricultural Imagery Program (NAIP) aerial photographs and ASTER thermal infrared (TIR) bands, which differentiate temperatures given off by glacierized and non-glacieriezed areas in the ablation area, were used to delineate the debris-covered ablation zone. The TIR subsystem of ASTER consists of five bands taken from one fixed-position, Nadir-looking telescope. It is the only subsystem of ASTER that has a scanning mirror system, but as a result, its resolution is limited to 90 meters (NASA, 2004). In the end, this resolution proved to be too coarse and was deemed ineffective in delineating the widths of Mount Hood glaciers. Therefore the combination of NAIP photographs and GPS (Global Positioning System) recordings taken on September 14, 2007, were consulted in the delineations of debris-covered ice.

NAIP imagery is acquired by aircraft and is available for most of the United States. PAN sharpening of color bands yields a 1 m resolution of ground sampling

distance. It has a horizontal accuracy that matches within 5 m of referenced orthorectified imagery (National Agricultural Imagery Program, 2006).

September 2005 NAIP aerial photographs coupled with a September 10, 2006 ASTER DEM and GPS-recorded glacier perimeters were used to generate a ratio (Band 3:4) minimum threshold of 2.0 for clean, debris-free glaciers. All connected pixels in the Coe and Eliot glacier areas were queried and all four data layers were consulted to manually digitize the debris-covered sections of the glaciers. These steps are outlined in Figure 3.2.

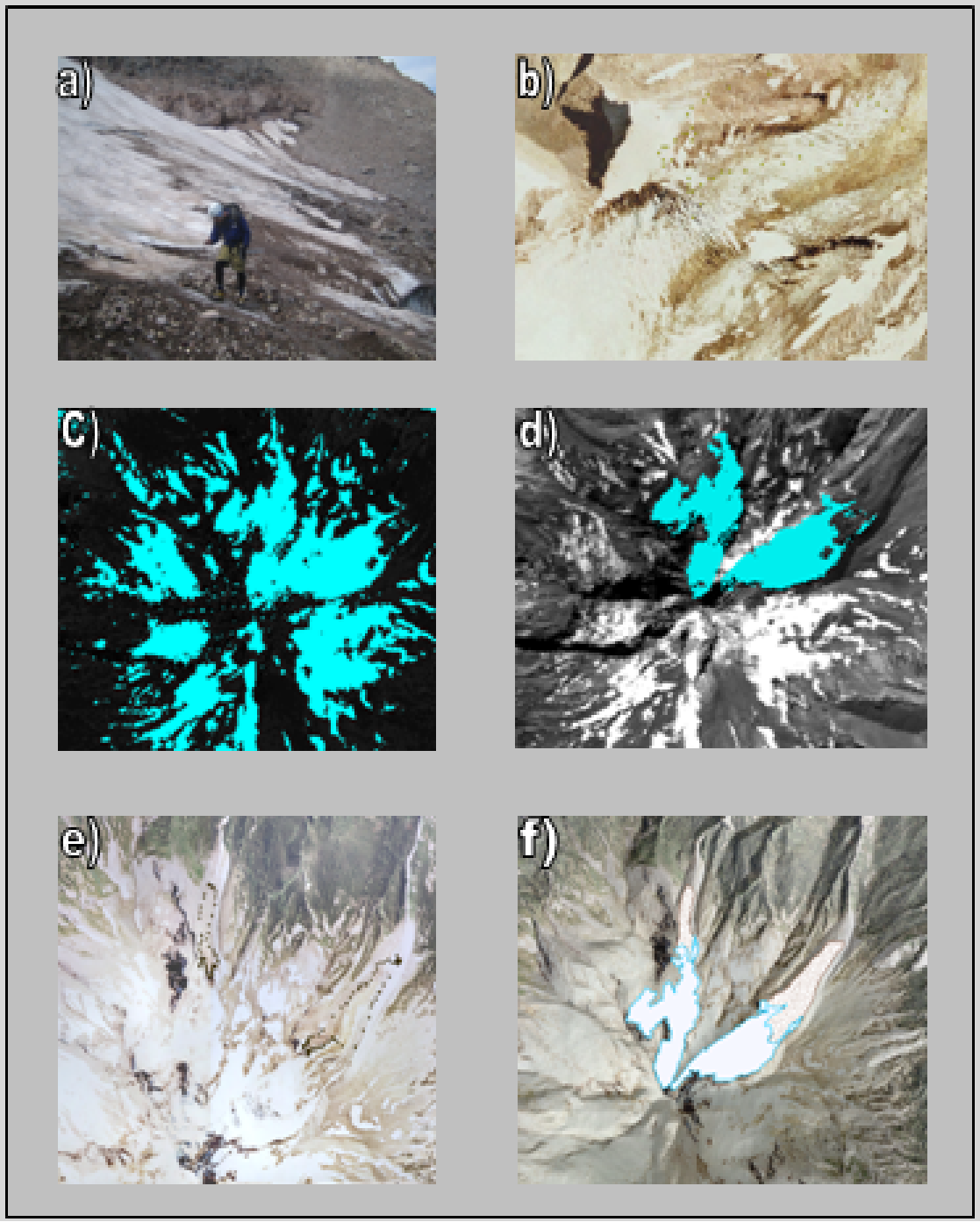

Figure 3.2. Steps taken for total glacier delineation for Eliot and Coe Glaciers: a) GPS measurements at the ice-debris boundary of Eliot Glacier, b) Threshold generation of ASTER B3/B4 image (September 10, 2006) using aerial photographs and GPS boundaries, c) Threshold Return in ENVI, d) ROI Intersect using specific glacier coverages which exclude lone pixels, e) Delineation of debris-covered glaciers using aerial photos for lateral extent and GPS coordinates for terminal extent, and f) Digitized shapefiles in ArcMap for both clean and rock glaciers

3.2 Model Input Parameters

3.21 *Catchment Area*

SRM was run for three high-altitude sub-catchments of the Upper Middle Fork Hood River: Coe, Eliot, and Compass (Figure 3.3). Each catchment was delineated using ArcHydro™ tools according to Appendix B.

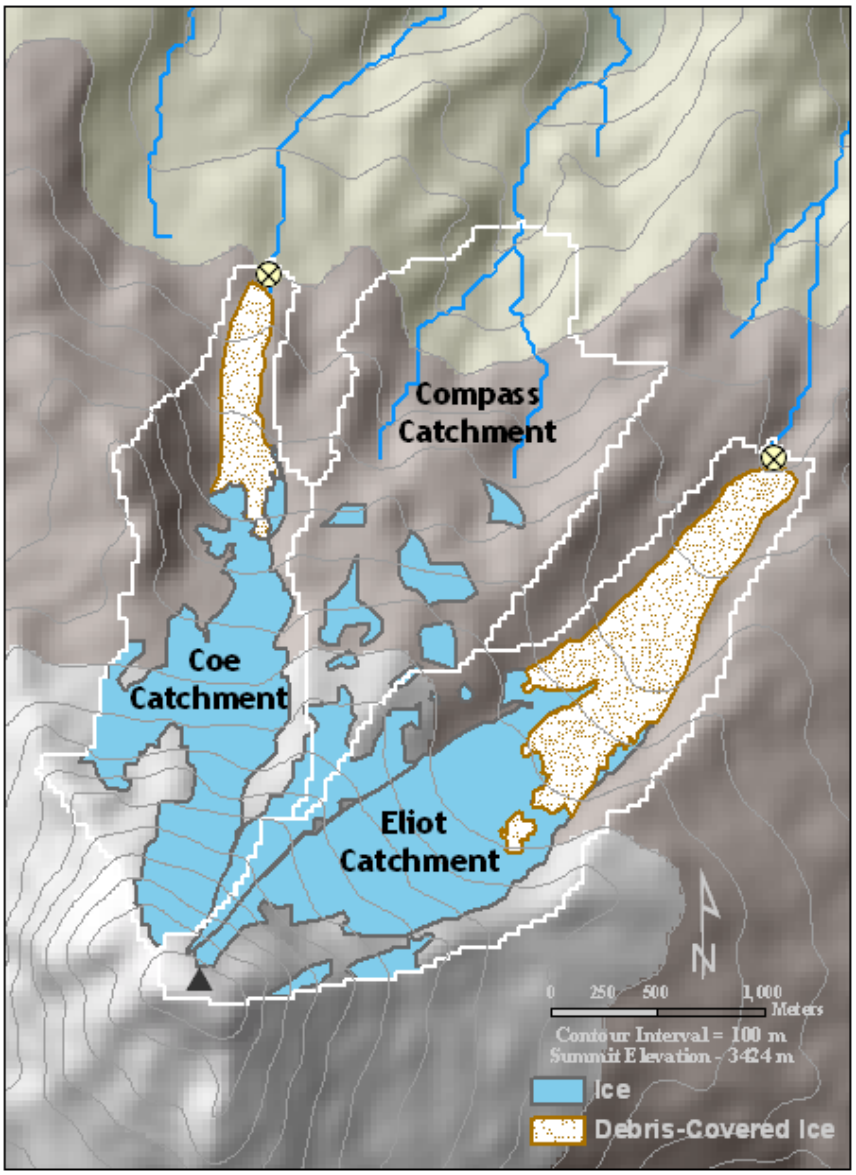

Figure 3.3 Location Map for the three glaciated catchments of the Upper Middle Fork Hood River. Each catchment was independently run in SRM. Locations of water height recorders are indicated by the yellow circles.

3.22 *Elevation Zones*

SRM is a semi-distributed model and requires variable inputs into specified elevation zones. The basin was divided into eight 200-meter elevation zones for the Eliot (Figure 3.4) and Coe catchments and five for the Compass catchment. SRM also requires the delineation of catchment area, percentage glacier cover, and hypsometric means for each elevation zone. The methods for generating these values are outlined in Appendix C.

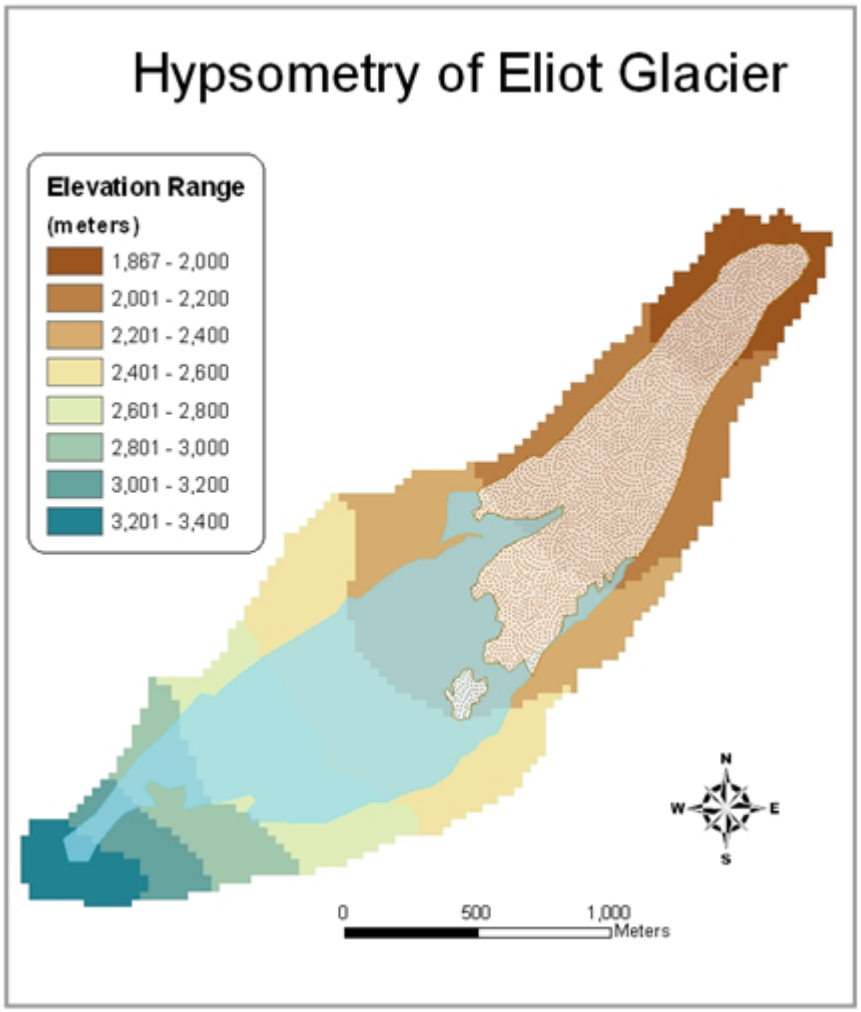

Figure 3.4 Elevation zones that were used for SRM input parameters for the Eliot Glacier catchment

3.23 *Temperature and Precipitation Lapse Rates*

A standard temperature lapse rate of 0.65°C/100 m was applied because this value has been shown to be a reasonable mean lapse rate for mountainous terrain (Barry, 1992). The precipitation lapse rate was generated according to the differences of 10-year mean data for the months of September and August from the Mount Hood SNOTEL site (1646 m) and the Red Hill SNOTEL site (1341 m). This lapse rate of 6.4%/100 m was manually applied into each elevation zone because the current version of SRM does not include a precipitation lapse rate calculation.

3.24 *Temperature vs. Glacier Meltwater Discharge Lag Time*

The termperature/glacier meltwater discharge lag time can be directly determined from historical hydrographs as the mean period between daily temperature rises and discharge increases (Martinec and Rango, 2007). Eliot Glacier stream discharge data coupled with hourly temperature data from Mount Hood Meadows ski area (Figure 3.5) indicate a lag time of 3 hours and 1 minute. The Coe Glacier stream discharge lag time was computed to be 3 hours and 15 minutes.

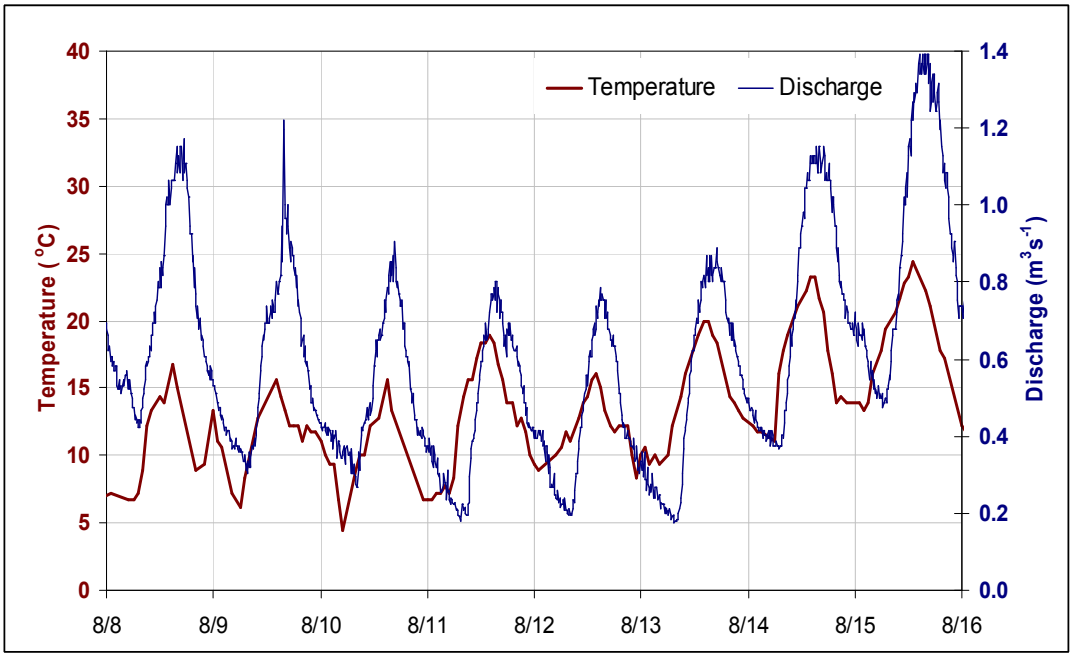

Figure 3.5 Lag time for temperature and discharge increases at the terminus of Eliot Glacier, August, 2007. Mean period between peaks = 2 hrs, 35 min; mean period between temperature and discharge initiation = 3 hrs, 29 min; mean lag time = 3hrs, 1 min.

3.25 *Degree Day Factor*

The Degree Day Factor (DDF) is typically measured empirically through the use of ablation stakes or a snowmelt lysimeter, mathematically with an energy-balance equation (Zhang et al., 2006a), or is computed according to its relationship to snow density (Martinec, 1960). Since Mount Hood meteorological stations lack wind and solar radiation measurements, an energy-balance computation is unrealistic, and the model relied on previous studies measuring the DDF on Mount Hood glaciers and other glaciers worldwide (Table 3.2). A mean DDF for snow (4.4 mm $^{o}C^{-1}$ d^{-1}) was applied to all zones above the Equilibrium Line Altitude (ELA), since this section of the glacier should be representative of that water year's snowpack. The mean DDF for ice (7.1 mm $^{o}C^{-1}$ d^{-1}) was applied to the ablation zone

above the debris-covered section of the glacier. This method of using the ELA as a boundary for the DDF was successfully used in a temperature-index model by Zhang et al. (2006b).

Table 3.2 Empirically-derived degree-day factors.

References	***Degree-Day Factor ($mm^0C^{-1}day^{-1}$)***	
	Ice	Snow
Kaser (1959)	5.0-7.0	--
Yoshida (1962)	--	4.0 - 8.0
Schytt (1964)	13.8	--
Orheim (1970)	6.3	--
Borovikova et al. (1972)	8.0	3.0-5.0
Anderson (1973)	--	1.3-3.7
Lang et al. (1977)	--	5.40
Braithwaite (1977)	5.5+/-2.3	--
Abal'yan et al. (1980)	8.0	5.0
Braithwaite (1981)	6.3+/-1.0	--
Braithwaite and Olesen (1988)	7.2	2.5
Woo and Fitzharris (1992)	6.0	3.0
Johannesson et al. (1995)	7.7	5.6
Johannesson et al. (1995)	6.4	4.4
Laumann and Tech (1993)	6.4	4.5
Laumann and Tech (1993)	5.5	4.0
Laumann and Tech (1993)	5.5	3.5
Braithwaite (1995)	8.0	--
Singh and Kumar (1996)	--	5.9
Singh et al. (2000)	7.3-8.0	5.8-6.4
Zhang et al. (2006)	7.1	4.1
Mean DDF	**7.1**	**4.4**

The ELA represents the elevation between the previous year's snow and glacier ice on the glacier at the end of the ablation season. Thus, it is easily interpreted in September photographs before snow begins to accumulate again. Although a transient snow line (TSL) may better suit the model because it changes elevation over the course of a season, the boundary change between snow and ice is likely negligible during the 2-month study period. Analysis of photographs by the author and NAIP (2005) aerial photographs generated an ELA for Eliot Glacier to be

approximately 2300 m. The established accumulation area ratio (AAR) of 0.52 for Eliot Glacier (Lundstrom, 1992) was used to geometrically compute an ELA of 2336 m, just 36 m higher than aforementioned calculation. Coe Glacier's ELA was calculated to be 2230 m, and this value was extrapolated to neighboring glacierettes for input into the SRM.

The degree-day factor for ice covered in debris is particularly difficult to compute (Hochstein et al., 1995). Kayastha et al. (2000) used a combination of in situ measurements and energy balance equations to calculate a negative relationship between thickness of debris cover and ablation rate for glaciers in Nepal. The ablation rate peaked under a debris cover of 0.3 cm and became negligible under a debris thickness of 1 m. Although this specific relationship is important, Kayastha et al. (2000) emphasize that each debris layer has its own thermal resistance, and there is ablation variability for different mountain ranges.

Fortunately, recent debris-cover ablation measurements in the study area are available. Jackson (2007) used stakes to calculate specific ablation rates for many parts of the debris-covered zone of Eliot Glacier. Although the degree day factors are not specified, he measured the ablation rate of a clean section of glacier so that the effect of debris insulation can be inferred. In Figure 3.6, he shows a strong correlation between ablation rate and distance downglacier from the clean glacier/debris-cover interface. This relationship is expected because the debris thickens downglacier and can more effectively insulate the underlying ice.

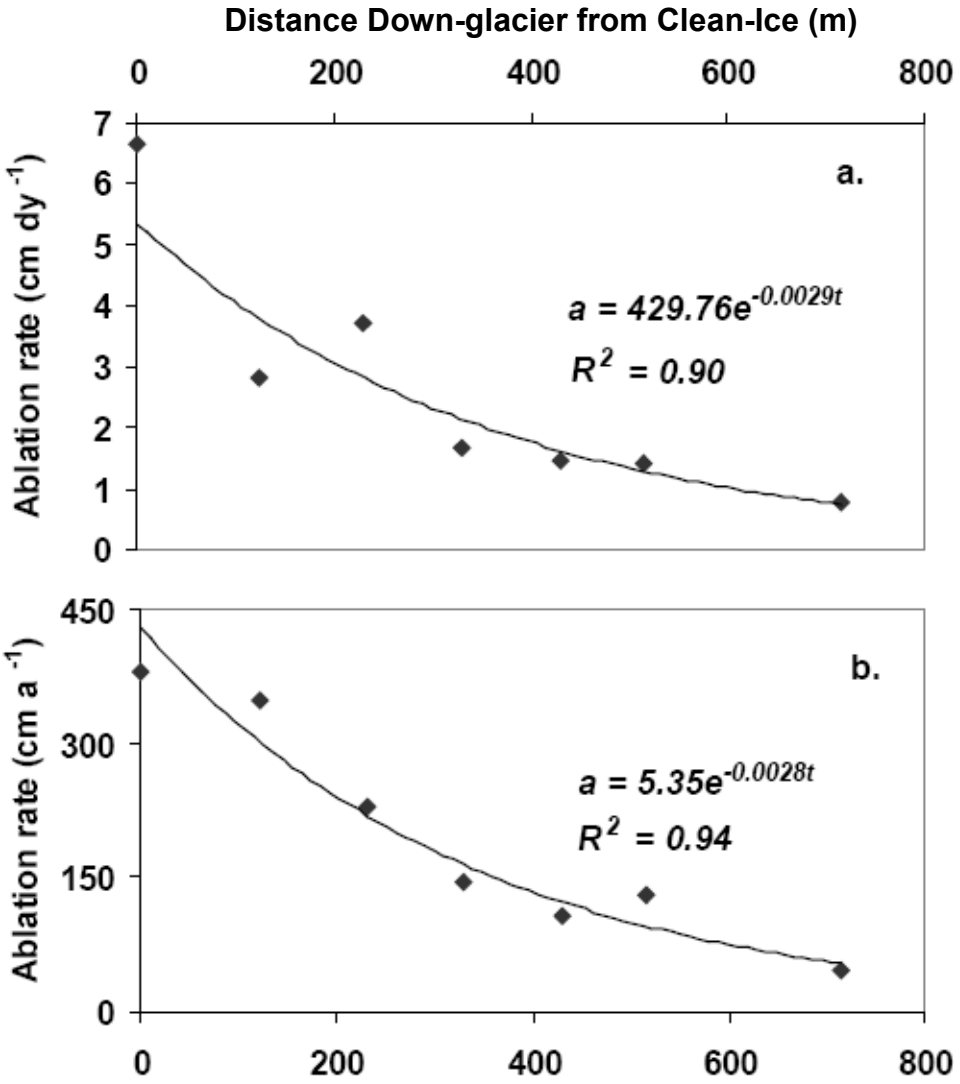

Figure 3.6 Ablation rates for stakes placed on the debris surface of Eliot Glacier in 2004. The x-axis represents the distance downglacier from the clean ice/debris-cover interface. The upper graph's measurements were taken between August 13-September 24, 2004 and the lower measurements were extrapolated from a 350-day period (Jackson, 2007).

Since the degree day factor is equal to the ablation rate divided by the number of degree days, one can spatially extrapolate degree day factors for areas that have a known ablation rate. This is shown in Equation 3.1:

$$\frac{Ai}{DDFi} = \frac{Ax}{DDFx} \qquad (3.1),$$

where Ai is the known ablation rate of an ice surface, DDFi is the known degree day factor of the ice surface, Ax is the known ablation rate of debris-covered ice, and DDFx is the unknown degree day factor for debris-covered ice.

Since the DDF for debris-covered ice varies with varying thickness of debris, it is necessary to spatially distribute the DDF according to measured sediment depths. These depths have been mapped by Jackson (2007) and other researchers in Figure 3.7.

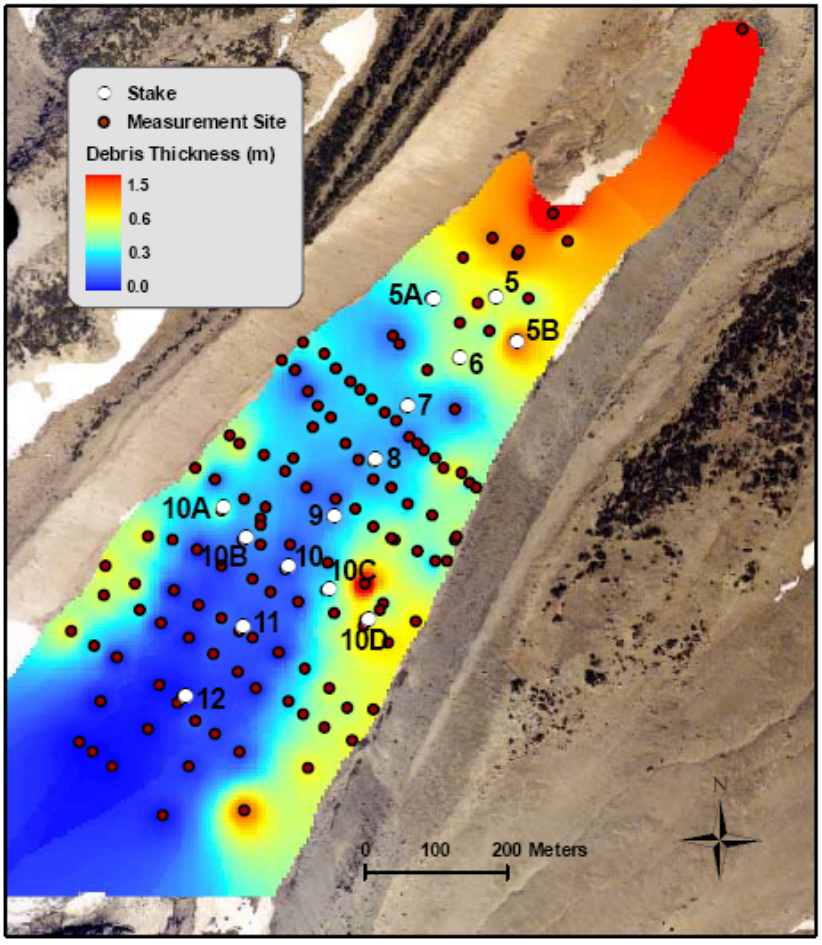

Figure 3.7 Debris thicknesses at the base of Eliot Glacier (Jackson, 2007).

Using the ablation-debris thickness relationship shown in Figure 3.6, ablation distribution was calculated throughout the glacier, and a mean value was applied to

each SRM zone. Scaled DDFs, calculated according to Equation 3.1 served as input parameters into the SRM. Because there is no thickness data available for the Coe Glacier, the mean thickness was assumed to be the same as Eliot (36 cm; Lundstrom, 1992) and one DDF was applied to the entire section of the debris-covered glacier. The mean DDF of glacier ice (Table 3.2) was applied to the debris-free ablation zone and the mean DDF for snow (Table 3.2) was applied to the accumulation zone. A spatially weighted mean DDF was calculated for SRM zones that contained more than one DDF value. When scaling back the DDFs for each glacier recession scenario, the overall weighted mean DDF for the glacier was kept to equal the weighted mean DDF for the original glacier. This served as confirmation that the DDF was accurately measured for each portion of the glacier, including the accumulation zone, the ablation zone, and the debris-covered zone. These DDF values are shown in Appendix D.

3.26 *Rainfall Contributing Area*

In SRM, the Rainfall Contributing Area (RCA) can have a value of one or zero. Early in the melt season, rain can be absorbed and stored by the snowpack (option zero). Later in the season, when the snowpack is ripened (option one), a rain event will trigger runoff from the snowpack that is equal in volume to the total precipitation during the event (Martinec and Rango, 2007). Option one was appropriate to this simulation because this study investigates the last two months of the water year, when glacier ice is exposed and snow is at its most ripened stage.

3.27 *Runoff and Recession Coefficients*

SRM requires a runoff coefficient for both rain and snowmelt. A runoff coefficient indicates the proportion of rain and snowmelt that is lost to infiltration, evapotranspiration, and sublimation, with a value of one yielding no losses and zero yielding 100% losses. Local runoff coefficients can be calculated by comparing historical precipitation data with historical discharge data. However when precipitation is poorly measured and there is limited historical data, the runoff coefficients commonly serve as adjustable parameters in the calibration process (Martinec and Rango, 2007). Since there are no historical precipitation or discharge data in the Upper Middle Fork, the rain and snowmelt runoff coefficients were calibrated for August and September of 2007 and are provided in Appendix E.

The recession coefficient, like the runoff coefficient, requires long-term discharge data in order to discern hydrograph characteristics following precipitation and snowmelt events. Because the falling limbs on the late season Upper Middle Fork hydrographs are interrupted by the next day's melting events, calculating the x- and y-coefficients of recession proved impossible and were therefore calibrated in the model instead (Appendix E).

3.29 *Precipitation Threshold*

The precipitation threshold is a SRM feature that increases the recession coefficient whenever there is a precipitation event that exceeds a user-specified depth (Martinec and Rango, 2007). The precipitation threshold was set to the minimum 0 value because, as justified by hydrograph responses to rain events, runoff in these small glaciated catchments is peaked and immediate. This application is especially

important when applied to the run using 27-year long-term average precipitation data. The problem of using mean precipitation is that short-term intense events are smoothed out into month-long light-intensity rain. If a high precipitation threshold value had been applied, then much of this rain would have been stored as groundwater, and not expressed as runoff during the August-September period. Setting the threshold to zero meant that precipitation would immediately contribute to surface runoff, a catchment behavior that became evident during the calibration process.

3.3 Model Calibration

The Snowmelt Runoff Model for the Eliot catchment was calibrated with Eliot Glacier discharge data from August 1, 2007 – September 29, 2007. Runoff coefficients and recession coefficients were modified to simulate the actual daily trends in runoff. The calibration was deemed successful with a reasonable coefficient of variation (r^2) of .89 and a total volume difference of 0.4% (Figure 3.8). All of the specific calibration parameters and variables are shown in Appendix E.

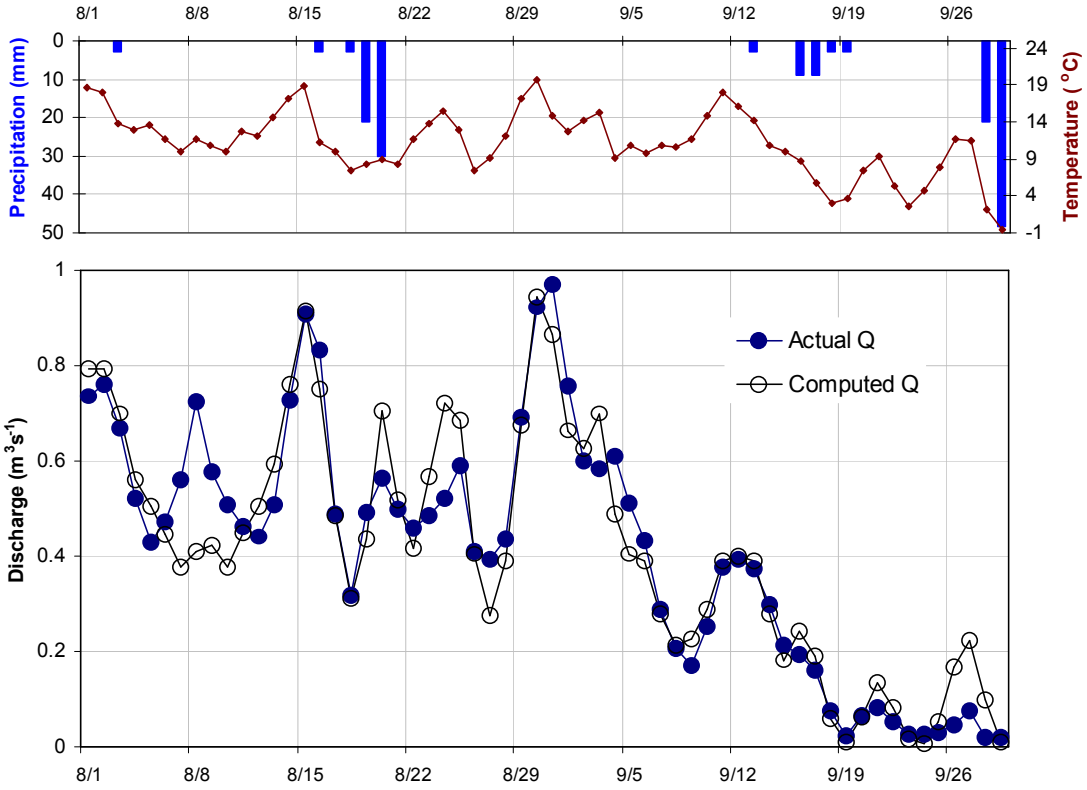

Figure 3.8 SRM calibration using the Eliot Glacier catchment: 8/1/07 – 9/29/07. r^2=0.89; total volumetric difference=0.4%

Chapter 4: Results

4.1 Discharge Measurements

Between 8/10/07 and 9/7/07, Coe and Eliot Creeks comprised 50.0% and 25.9% of all surface runoff in the Upper Middle Fork catchment, respectively, and exhibited extreme diurnal variations (Figure 4.1). With no glacier inputs, Clear and Pinnacle Creeks showed minimal variation in the daily cycle of discharge and contributed 11.1 and 4.0% of the total catchment runoff. Unlike the glacier-fed creeks, Clear Creek was much more responsive to precipitation events than warming events. According to upstream measurements (Figures 4.2 and 4.3), Eliot and Coe glaciers released 40.8% of the catchment's discharge during this period. The Eliot Creek supplied 88% of the total meltwater. This contribution, however, does not include the isolated glacierettes of the Compass catchment which feed into Coe Creek.

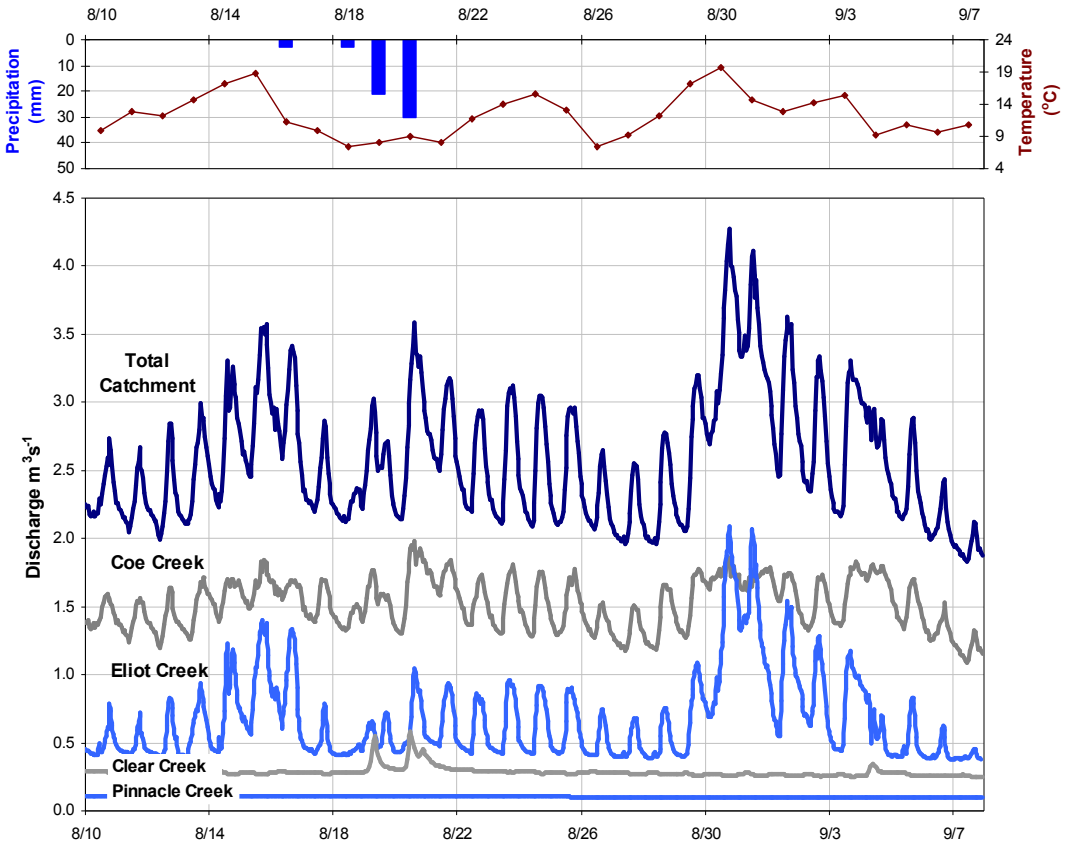

Figure 4.1 Upstream contributions to the Upper Middle Fork Hood River: 8/10/01 - 9/7/07. Temperature and precipitation were recorded at an elevation of 1600 m and at a distance of 1.8 km from the catchment.

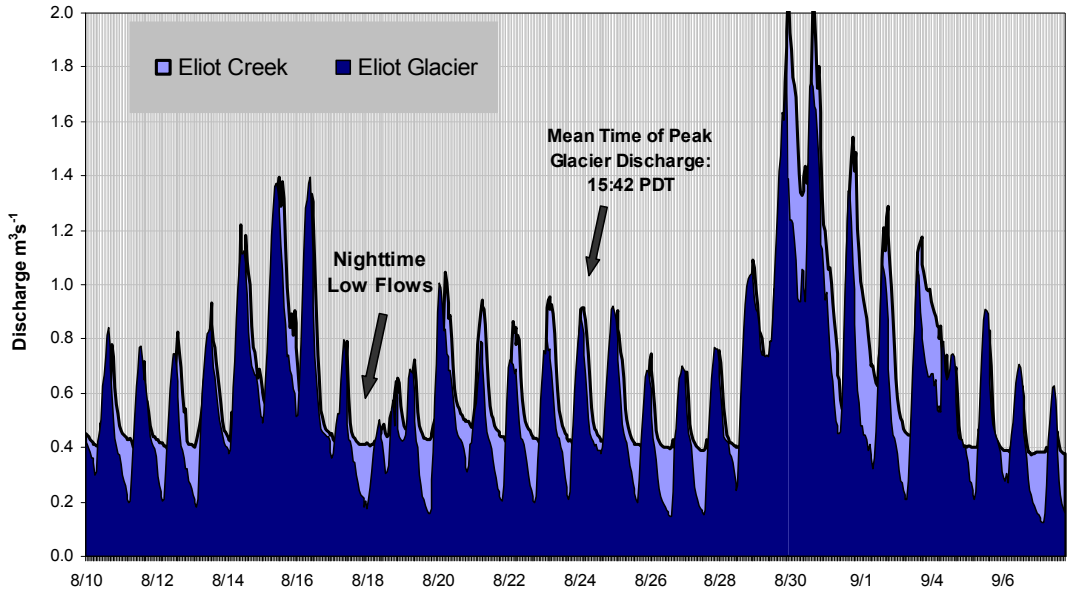

Figure 4.2 Glacier and total runoff on the Eliot Creek: 8/10/07 – 9/7/07.

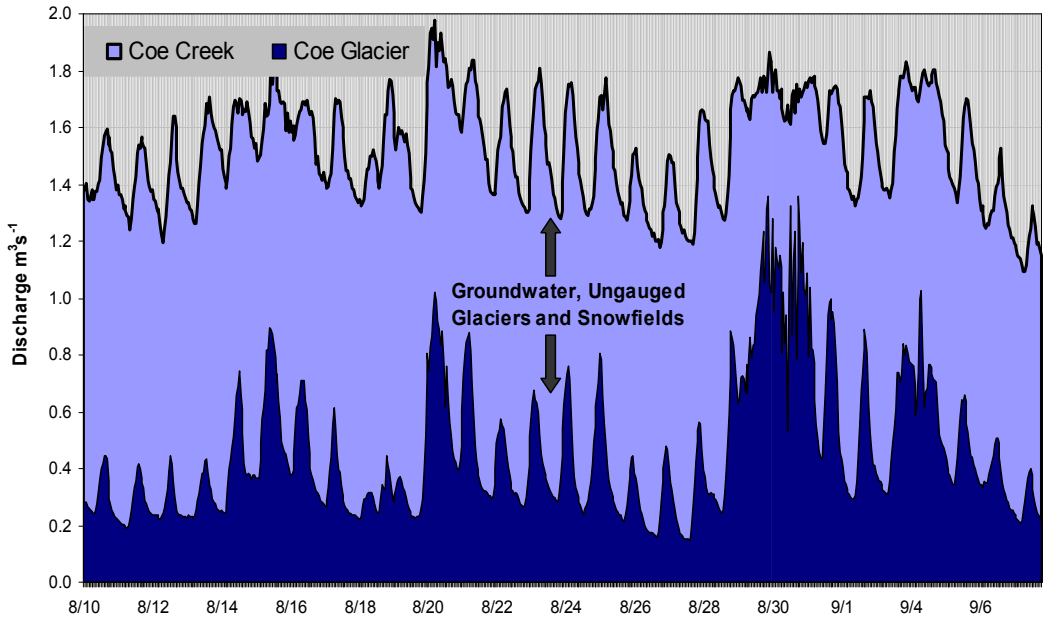

Figure 4.3 Coe Glacier and Coe Creek runoff: 8/10/07 – 9/7/07.

To physically compare the hydrological patterns of glacier discharge with creek discharge, the Eliot Glacier hydrograph was stacked with that of the lower Eliot Creek for a five-day period that bracketed an isotope sampling date (Figure

4.4). For ease of comparison, the Eliot Glacier discharge was lagged by 2.3 hours, which is the time difference between peak runoff for the two sites. Over the five days, glacier discharge represented between 47 and 98% of total runoff at a given time. The lowest discharges occurred in the early morning, a time when fractional contribution by the Eliot Glacier was minimal. Fractional contribution peaked during both the rising and falling limbs of the daily hydrographs. The two hydrographs are similar, except in the late evening when stream flow levels out sooner for the lower creeks than it does for glacier discharge.

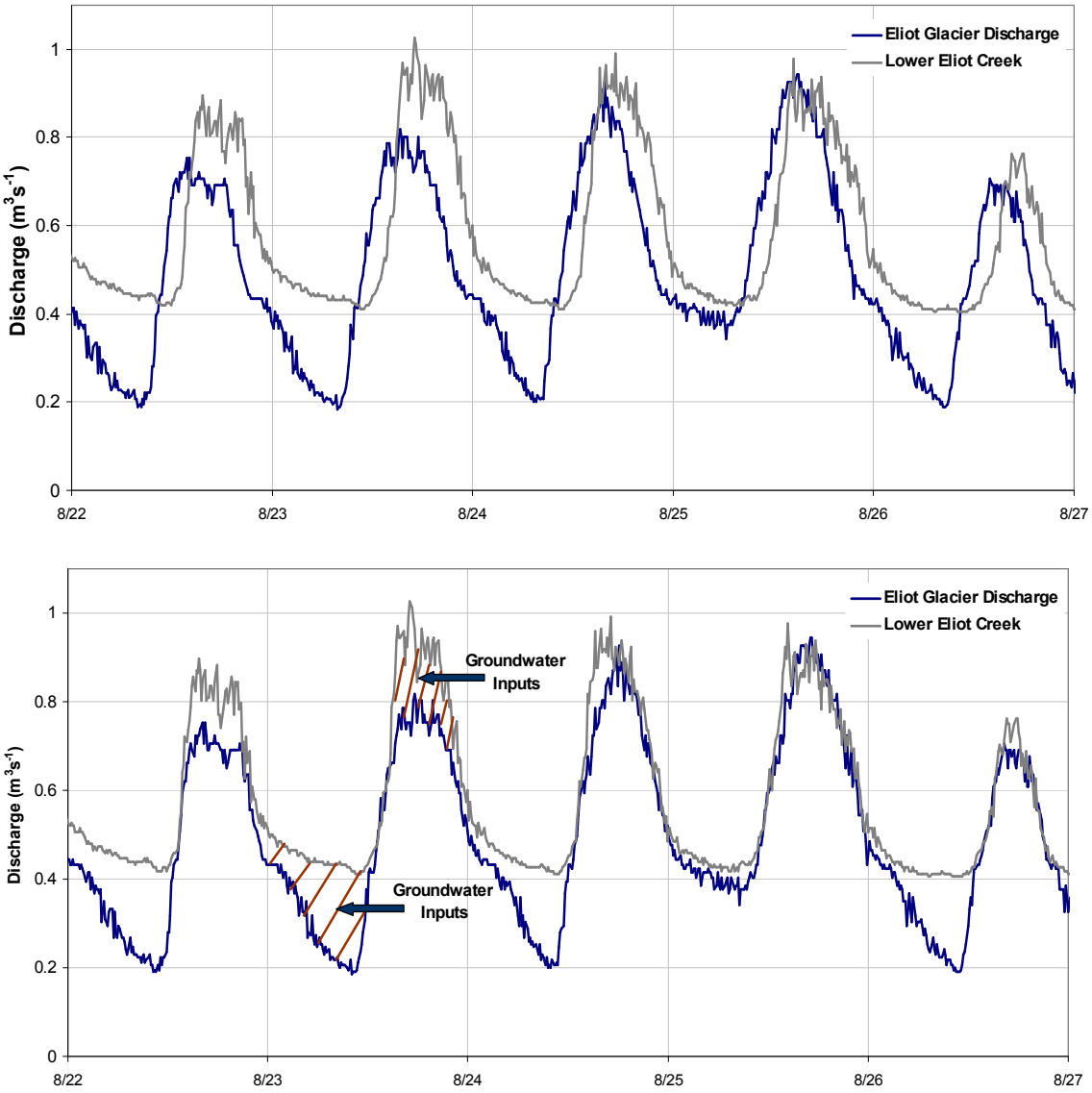

Figure 4.4 The Diurnal variation in both glacier Discharge and Terminal Flow in Eliot Creek: August 22 – 27, 2007 (top). The lower histogram delays glacier discharge by 2 hours and 18 minutes to compare hydrograph geometries.

4.2 Isotope Analysis

Isotopic analyses show that in the Eliot and Coe catchments, glacier ice is most depleted in ^{18}O, followed by surface water and springs (Figure 4.5). Given the accuracy of isotope reporting ($^{+}$/- .03 permil), the differences in ^{18}O compositions are significant. The application of Equation 2.3 to sample data shows that glacier melt can contribute 76 – 88% of the runoff in Eliot Creek and 70 – 88% in Coe Creek (Table 4.1), totaling 62 – 74% of the entire catchment's discharge. The isotopic representation of glacier melt is much higher than that exhibited by the discharge method because the isotopes represent both the Coe Glacier and all of its neighboring glacierettes.

The measured contributions were compared between the two methods on July 24 at 17:12 PDT. At this time the falling limb of the Eliot Creek hydrograph was estimated to have an 88% glacier component by the tracer study and a 94% glacier component by the dual hydrograph analysis. Glacier discharge measured using the tracer method deviated from the dual analysis measurement by 6.7%.

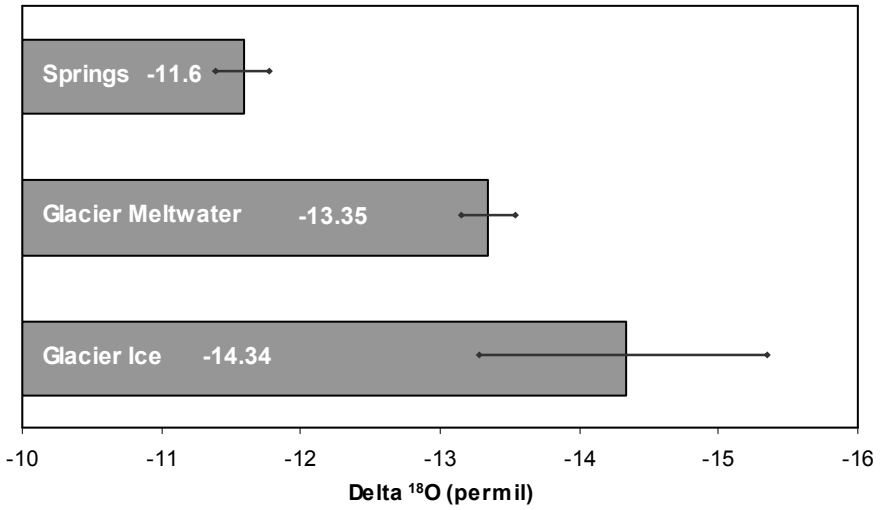

Figure 4.5 ^{18}O signatures of source water for the Upper Middle Fork Hood River. 24 samples were taken between 9/10/07 and 10/13/07 and are reported relative to SMOW. Error bars reflect $^{+}$/- .03 permil reporting accuracy and the standard mean error of the sample.

Table 4.1 The proportion of glacier melt in Eliot and Coe Creeks (2007), generated from a 2-component Oxygen-18 mixing model. Times are in PDT and error range was calculated according to $^{+}$/- .03 permil accuracy of isotope reporting.

	Glacier Melt
Eliot Creek	**Contribution (%)**
8/24 17:12	87.7 $^{+}$/- 4.0
9/14 7:47	77.6 $^{+}$/- 3.2
10/13 21:57	75.7 $^{+}$/- 2.6
Coe Creek	
8/24 13:30	87.7 $^{+}$/- 5.4
9/11 22:10	70.2 $^{+}$/- 6.4

4.3 Modeling Results

4.31 *Debris-Covered Area of Glaciers*

Coe and Eliot Glaciers are mapped (4.6) and their respective component areas are calculated (Table 4.2). United States Geological Survey (USGS) Quads (1956) missed more than 60% of the debris-covered glacier area (Figures 4.6 and

4.7) but overestimated glacier coverage in other areas, likely due to the time of year and age of the referenced photographs. If one were to solely consult the ASTER band ¾ ratios in the delineation of Eliot, then there would be more than 40% underestimation of glacier area.

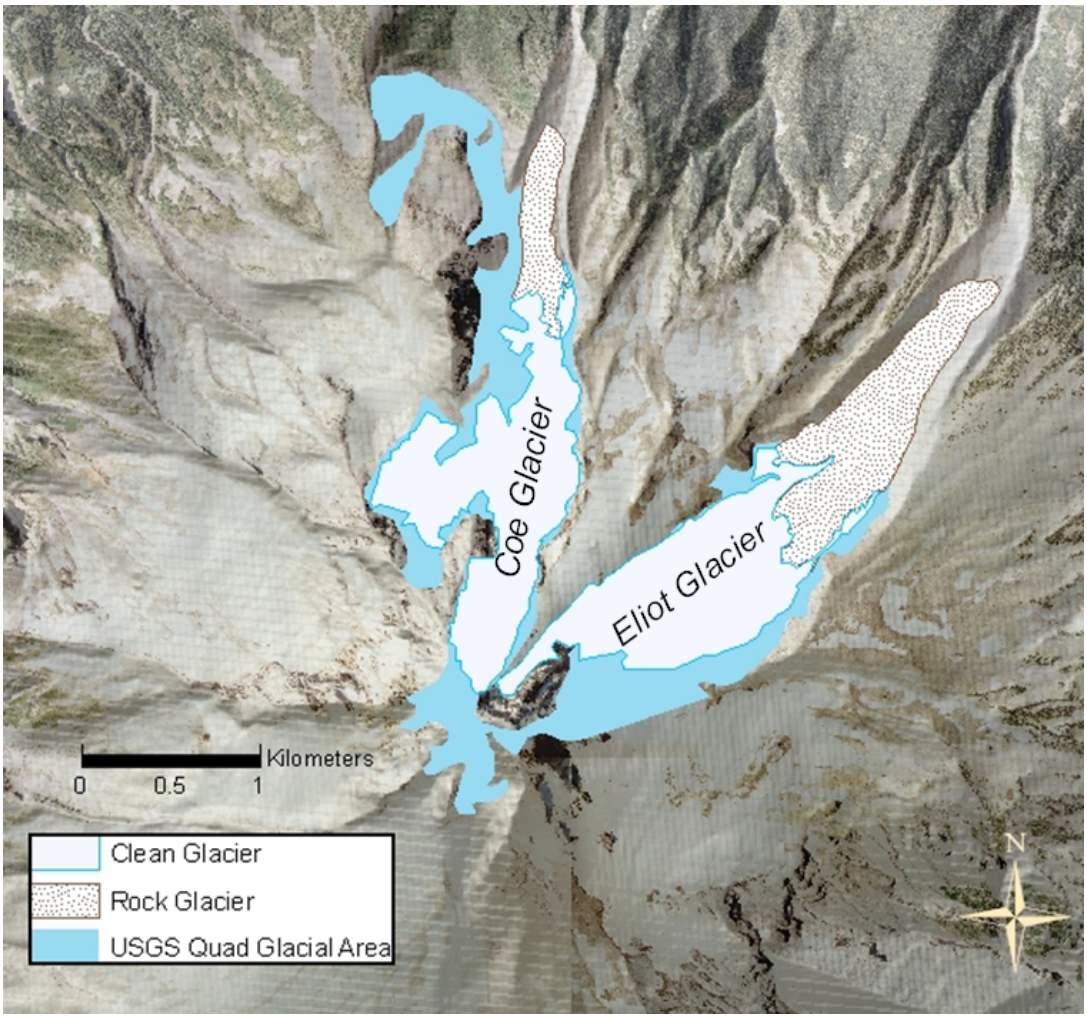

Figure 4.6 Glacial Components of the Coe and Eliot Glaciers – Mt. Hood. The debris-covered glaciers were delineated with aerial photographs coupled with a DEM, while the clean glaciers were measured with ASTER 3 / 4 bands (threshold=2.0).

Table 4.2 Glacier areas derived using ASTER imagery and GPS recordings (2007)

Glacier	Total Area (km^2)	USGS Area (km^2)	Debris-Covered Area (km^2)	Debris Cover (%)
Eliot	1.61	1.67	.67	41.6
Coe	1.26	2.11	.20	16.2

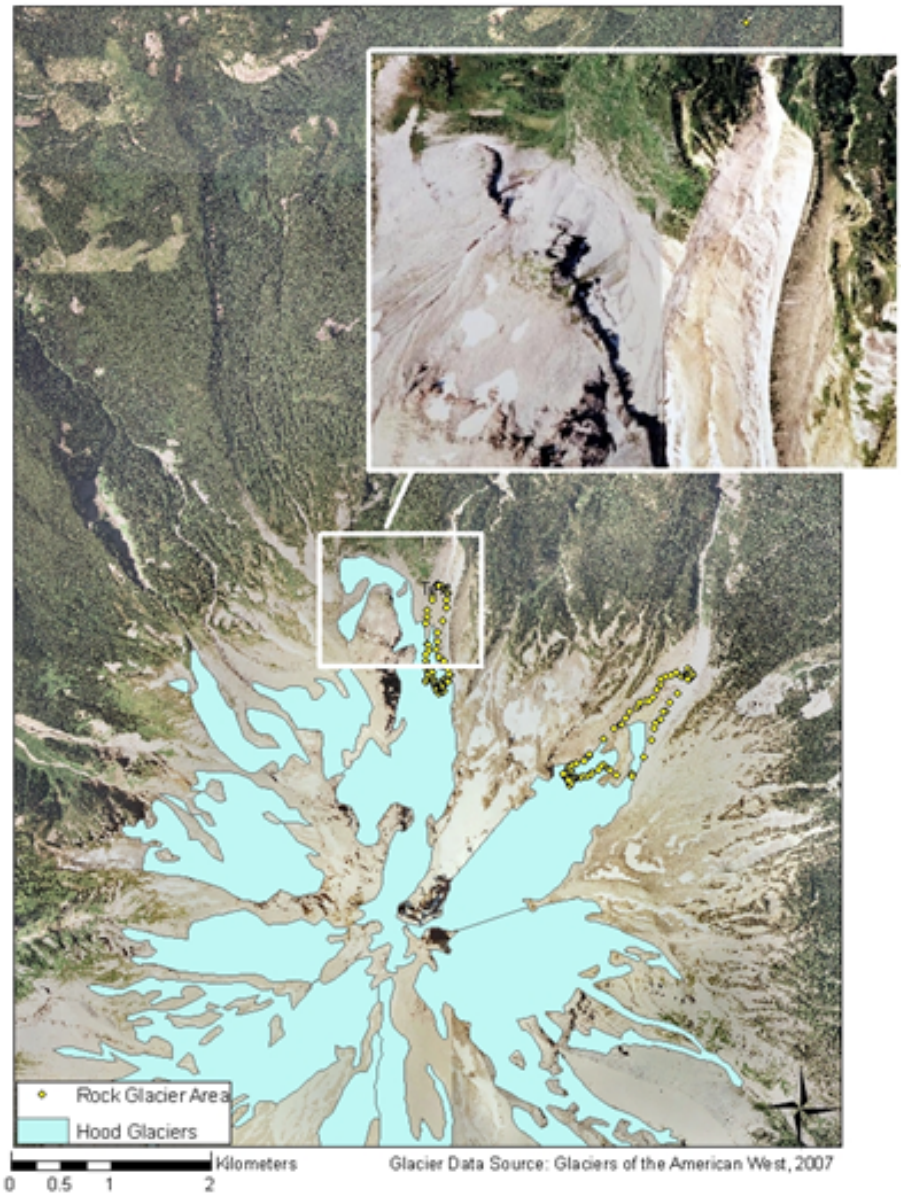

Figure 4.7 The clear misrepresentation of the Coe Glacier by a USGS Quad. The yellow dots are in situ GPS recordings and delineate the debris-covered sections of Coe and Eliot Glaciers. The blue glaciers are taken from a 1956 photo-referenced USGS Quad, which like many other quads, still serve as the spatial input for glacier databases worldwide.

4.32 *Model Validation*

Validation was assessed according to the Nash-Sutcliffe model efficiency coefficient. Developed by Nash and Sutcliffe (1970), the coefficient has become the standard statistic to gage the predictive ability of hydrologic models. It is measured as:

$$R^2 = 1 - \frac{\sum_{i=1}^{n} (Q_i - Q_i')^2}{\sum_{i=1}^{n} (Q_i - \overline{Q})^2} \qquad (4.1)$$

where:

Q_i is the measured daily discharge

Q_i' is the computed daily discharge

$\overline{Q}$ is the average measured discharge of the given year or snowmelt season

n is the number of daily discharge values

(Nash and Sutcliffe, 1970)

Nash-Sutcliffe coefficients can vary between -∞ and one, whereby one indicates a perfect match between discharge and simulated results, and zero indicates that the simulations are only as accurate as the observed mean of the data (Nash and Sutcliffe, 1970). Analogous to the R^2 coefficient of determination used in other statistical models, a value closet to one is ideal.

The total volumetric difference (D_v) between simulated and measured runoff was used as a secondary accuracy criterion for the model, as expressed in the equation below:

$$D_v = \frac{V_R - V'_R}{V_R} \cdot 100 \qquad (4.2)$$

where D_v is the percentage difference between the model simulation and measured values, V_R is the measured runoff volume, and V'_R is the modeled runoff volume (Martinec and Rango, 1989). The simulated cumulative runoff is a perfect approximation when D_v is equal to zero.

SRM validation (Figure 4.8) was performed using the same calibrated parameters from the calibration process (Appendix D). A validation run was applied to the Coe Glacier Catchment, using discharge data from 8/10/07 to 9/27/07. This yielded a Nash-Sutcliffe coefficient of 0.81 and a 5.43% volumetric difference between the simulated and the measured values for the entire time period.

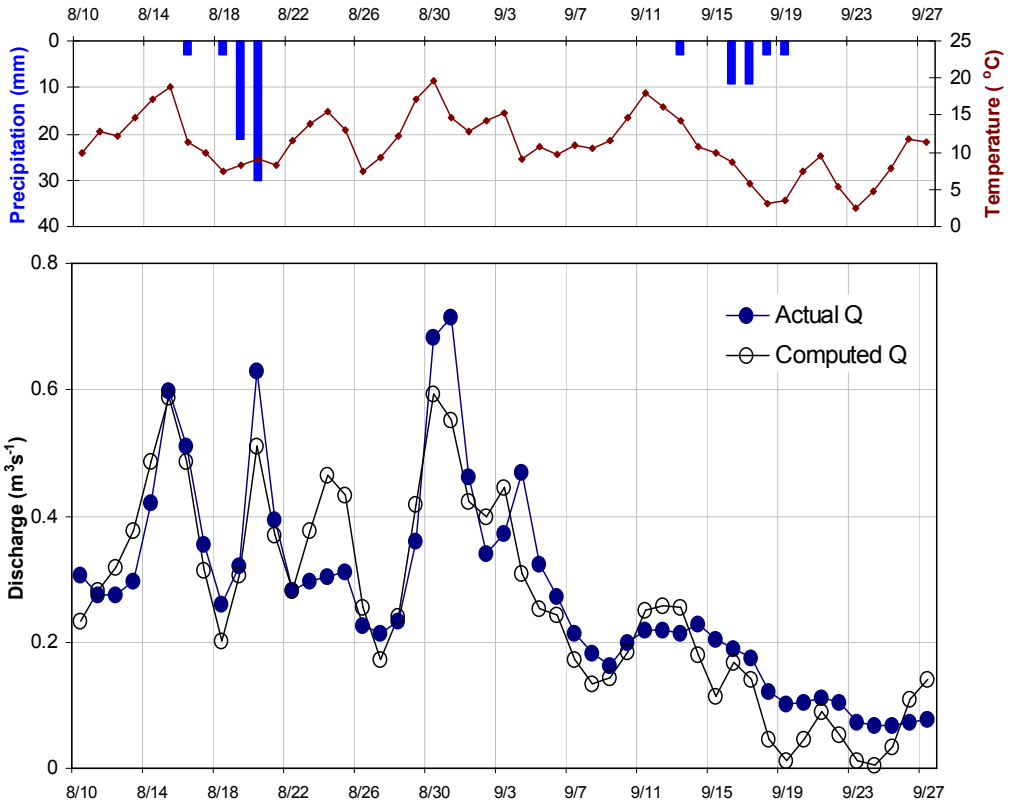

Figure 4.8 SRM validation using the Coe Glacier catchment: 8/10/07 – 9/27/07. r^2 = 0.81; total volumetric difference = 5.43%.

4.33 *Current Glacier Meltwater Discharges*

Applying 25-year mean temperature and 27-year mean precipitation values to the calibrated SRM, the current mean discharges were modeled for the months of August and September (Figure 4.9) for each of the three glacier catchments. With the highest fraction of glacier cover, the Eliot glacier expectedly has the highest total runoff for the time period, whereas the Compass Catchment has the lowest. The differences in discharge for each catchment become smaller in September as temperatures decline and precipitation becomes a major input to runoff.

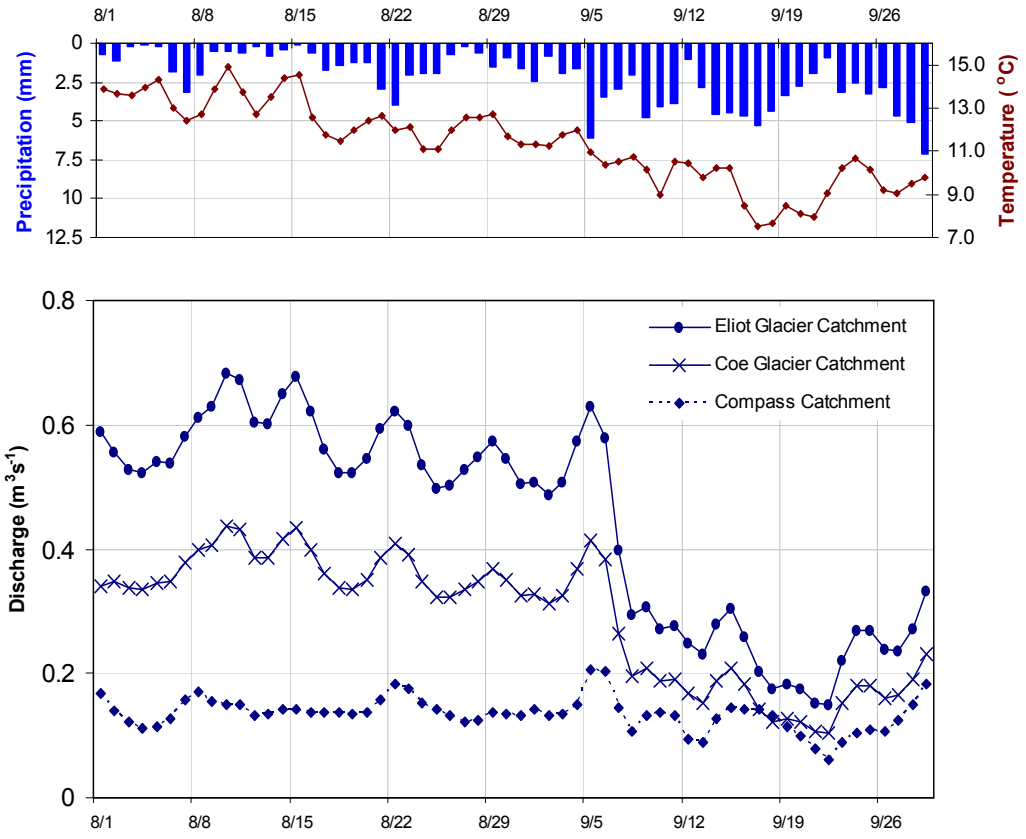

Figure 4.9 Modeled daily discharge for 2007 catchment conditions in the Upper Middle Fork of the Hood River. Applied meteorological variables include 25-year mean temperature and 27-year mean precipitation data from the Mount Hood SNOTEL site.

4.34 *Model Sensitivity – Debris Cover*

The retreat of Mount Hood glaciers has been well documented and recession rates have been proposed (Lillquist and Walker, 2006; Jackson and Fountain, 2007; Dodge, 1987; Driedger and Kennard, 1986; Lundstrom, 1992), however little is known about the rates of retreat of the debris-covered sections of Eliot and Coe Glaciers. Because debris cover significantly lowers the degree-day factor (Kayastha et al., 2000) of a glacier, the size of the debris-cover relative to the entire glacier is likely an important determinant in the overall glacier melt. To determine the model sensitivity to the fraction of debris cover, SRM was run under 4 scenarios: 1) 2007 clean-glacier and debris-covered glacier zones, 2) 2007 glacier area with no debris-cover, 3) 50% glacier recession with proportionally scaled debris-cover from 2007 conditions, and 4) 50% glacier recession with no debris cover, all of which used 25-year temperature and 27-year precipitation means as meteorological inputs (Figure 4.10). The Eliot Glacier simulations proved to be highly influenced by the degree of debris cover (Table 4.3). If one were to overlook the 2007 fraction of debris cover for the Eliot and applied a uniform degree-day factor for the entire ablation zone, then the overall glacier melt would be overestimated by 41.3%. This overestimation decreases as the glacier recedes to higher elevations but still remains significant at 35.7%. The influence of debris cover is higher in August than it is in September for both scenarios.

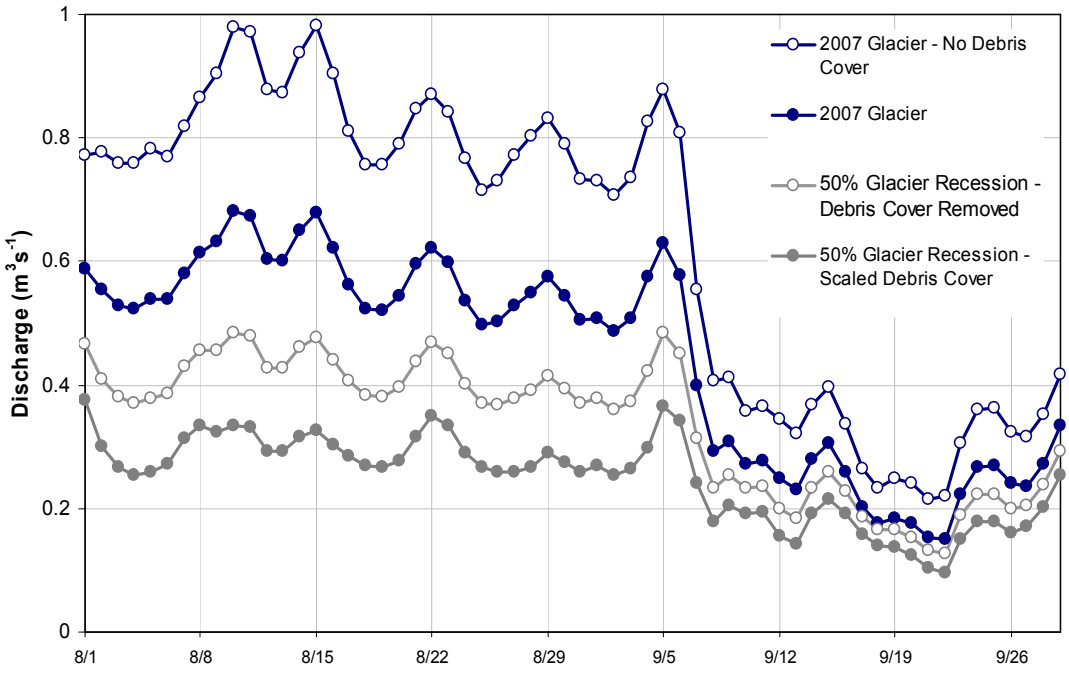

Figure 4.10 Debris Cover Sensitivity for Eliot Glacier. All meteorological inputs were based on 25-year temperature and 27-year precipitation daily mean data.

Table 4.3 SRM simulation results for the Eliot Glacier to investigate model sensitivity to debris cover: 8/1 – 9/29.

Scenario	Total Discharge (m^3)	Deviation from Debris-Covered State (%)
2007 Conditions	**2.32×10^6 m^3**	-
• August	1.54×10^6 m^3	-
• September	7.81×10^5 m^3	-
2007 Conditions – Debris Cover Removed	**3.28×10^6 m^3**	**41.3**
• August	2.21×10^6 m^3	**43.5**
• September	1.07×10^6 m^3	**33.3**
50% Recession – Scaled Debris Cover	**1.29×10^6 m^3**	-
• August	7.92×10^5 m^3	-
• September	4.96×10^5 m^3	-
50% Recession – Debris Cover Removed	**1.75×10^6 m^3**	**35.7**
• August	1.12×10^6 m^3	**41.4**
• September	6.34×10^5 m^3	**27.8**

4.35 *Model Sensitivity – Degree-Day Factor*

In this study, the degree-day factor was derived from the compiled mean of other DDF studies and served as the input parameters for the accumulation zones and debris-free ablation zones. Since these values were not directly measured in the study area, it was deemed necessary to run a sensitivity analysis of the DDF, again using the Eliot Glacier. The maximum documented DDF (Table 3.2) simulated a runoff response that was 21% greater than the discharge simulated by the mean DDF, whereas the minimum DDF yielded a total runoff that was 16% less (Table 4.4).

Table 4.4 SRM simulation results for the Eliot Glacier to investigate model sensitivity to the degree-day factor: 8/1 – 9/29

Scenario	Total Discharge (m^3)	Deviation from Mean DDF (%)
2007 Conditions – Mean DDF	**2.32×10^6 m^3**	-
• August	1.54×10^6 m^3	-
• September	7.81×10^5 m^3	-
2007 Conditions – Minimum Degree-Day Factor	**1.83×10^6 m^3**	**21.1**
• August	1.18×10^6 m^3	**23.3**
• September	6.50×10^5 m^3	**12.0**
2007 Conditions – Maximum Degree-Day Factor	**2.68×10^6 m^3**	**15.5**
• August	1.81×10^6 m^3	**17.5**
• September	8.75×10^5 m^3	**12.0**

4.36 *Model Sensitivity – Elevation Zones*

A sensitivity analysis was run to measure the effect of changing the number of and the classification of elevation zones in SRM. A simulation using 16 elevation zones instead of the eight used in this study yielded minimum changes in discharge (<1%), while the use of four elevation zones yielded a deviation of 2.2% (Table 4.5). Reclassifying the zones so that they all had equal catchment area, instead of equal

200-meter elevation intervals, also showed minimal changes in total discharge (<1%).

Table 4.5 SRM simulation results for the Eliot Glacier to investigate model sensitivity to elevation zone inputs: 8/1 – 9/29

Scenario	Total Discharge (m^3)	Deviation from 8 Equal Elevation Zones (%)
8 200-meter Elevation Zones*	**2.32×10^6 m^3**	-
• August	1.54×10^6 m^3	-
• September	7.81×10^5 m^3	-
8 Equal Area Elevation Zones	**2.31×10^6 m^3**	**0.43**
• August	1.53×10^6 m^3	**0.64**
• September	7.77×10^5 m^3	**0.5**
16 200-meter Elevation Zones	**2.31×10^6 m^3**	**0.43**
• August	1.53×10^6 m^3	**.64**
• September	7.75×10^5 m^3	**0.77**
4 200-meter Elevation Zones	**2.37×10^6 m^3**	**2.2**
• August	1.56×10^6 m^3	**1.3**
• September	8.06×10^5 m^3	**3.2**

*Used in this study

4.37 *Model Sensitivity – Temperature*

Model sensitivity to increased temperatures on the Eliot Glacier, was assessed both for current glacier area and for a 50% glacier recession, using long-term climate averages up until 2007 as the baseline inputs (Figures 4.11 and 4.12). According to Table 4.5, the mean incremental increase in discharge for each 1°C forcing on the 2007 glacier area is 5.3×10^3 $m^3°C^{-1}day^{-1}$, with increases being slightly smaller under greater temperature forcing scenarios. The effect of temperature increases is more pronounced for August than it is for September, yielding a mean increase in discharge of 6.29×10^3 $m^3°C^{-1}day^{-1}$, yet the percent of volume increase is less. For each 1°C forcing, there is a mean of 13.8% increase in total discharge volume for the two months combined. This forcing is greater than

that experience by the 50% glacier area simulation, which sees a mean of 12.6% increase in total discharge, and an increase in runoff of 2.52 m^3 $°C^{-1}day^{-1}$.

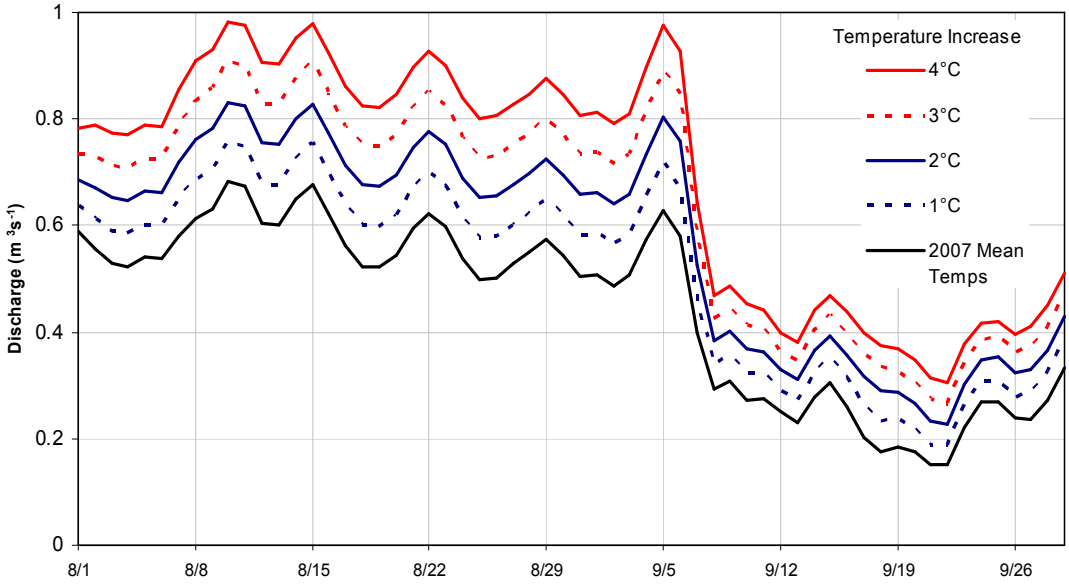

Figure 4.11 SRM Simulations for the 2007 Eliot Glacier with modeled temperature sensitivities.

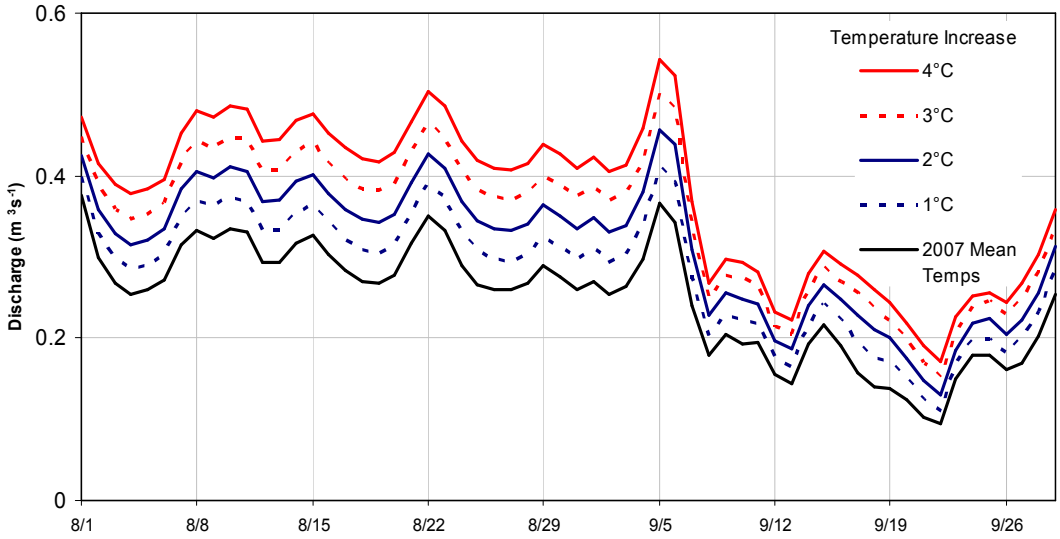

Figure 4.12 SRM Simulations for Eliot Glacier with temperature increases under a 50% glacier recession scenario. In this simulation, the debris-covered glacier is scaled proportionally to the glacier retreat.

Table 4.6 SRM simulation results for the Eliot Glacier to investigate model sensitivity to temperature forcings: 8/1 – 9/29.

Scenario	Total Discharge (m^3)	Discharge (m^3/°C/day)	Discharge Increase (m^3/°C/day)	Increase from 2007 Data (%)
2007 Glacier Area – Mean Temp.	**2.32×10^6 m^3**	3.87×10^4	-	-
• August	1.54×10^6 m^3	4.97×10^4	-	-
• September	7.81×10^5 m^3	2.69×10^4	-	-
2007 Glacier Area – 1°C Increase	**2.65×10^6 m^3**	4.42×10^4	5.50×10^3	**14.2**
• August	1.73×10^6 m^3	5.58×10^4	6.10×10^3	**12.3**
• September	9.16×10^5 m^3	3.16×10^4	4.70×10^3	**17.2**
2007 Glacier Area – 2°C Increase	**2.98×10^6 m^3**	4.97×10^4	1.10×10^4	**28.4**
• August	1.93×10^6 m^3	6.23×10^4	1.26×10^4	**25.3**
• September	1.05×10^6 m^3	3.62×10^4	9.3×10^3	**30.7**
2007 Glacier Area – 3°C Increase	**3.29×10^6 m^3**	5.48×10^4	1.62×10^4	**41.4**
• August	2.12×10^6 m^3	6.84×10^4	1.87×10^4	**37.7**
• September	1.17×10^6 m^3	4.03×10^4	1.34×10^4	**49.8**
2007 Glacier Area – 4°C Increase	**3.60×10^6 m^3**	6.00×10^4	2.13×10^4	**55.2**
• August	2.31×10^6 m^3	7.45×10^4	2.48×10^4	**50.0**
• September	1.29×10^6 m^3	4.45×10^4	1.76×10^4	**65.2**
50% Glacier Area – Mean Temp.	**1.29×10^6 m^3**	2.15×10^4	-	-
• August	7.92×10^5 m^3	2.56×10^4	-	-
• September	4.96×10^5 m^3	1.71×10^4	-	-
50% Glacier Area – 1°C Increase	**1.46×10^6 m^3**	2.43×10^4	2.8×10^3	**13.2**
• August	8.88×10^5 m^3	2.86×10^4	3.0×10^3	**12.1**
• September	5.70×10^5 m^3	1.97×10^4	2.6×10^3	**14.9**
50% Glacier Area – 2°C Increase	**1.63×10^6 m^3**	2.72×10^4	5.7×10^3	**26.4**
• August	9.84×10^5 m^3	3.17×10^4	6.1×10^3	**19.5**
• September	6.41×10^5 m^3	2.21×10^4	5.0×10^3	**29.2**
50% Glacier Area – 3°C Increase	**1.79×10^6 m^3**	2.98×10^4	8.3×10^3	**38.8**
• August	1.08×10^6 m^3	3.48×10^4	9.2×10^3	**36.4**
• September	7.07×10^5 m^3	2.43×10^4	7.2×10^3	**42.5**
50% Glacier Area – 4°C Increase	**1.94×10^6 m^3**	3.23×10^4	1.08×10^4	**50.4**
• August	1.18×10^6 m^3	3.81×10^4	1.25×10^4	**49.0**
• September	7.67×10^5 m^3	2.64×10^4	9.3×10^3	**54.6**

4.38 *Effect of Glacier-Covered Area on Melting and Runoff*

To investigate the glacier melt component of the SRM-generated hydrographs, simulations were run under drought conditions by holding precipitation to a constant zero value for all of the glacier catchments (Eliot, Coe, and Compass).

25-year temperature mean daily inputs coupled with the 2007 GCA outputted a discharge of 2.29 x 10^6 m^3 for the total runoff period. In ArcGIS, a geometrically-scaled GCA (Figure 4.13) was generated according to past recessional characteristics (Jackson, 2007). Therefore, the glacier width and glacier length were decreased at the relative rates indicated by previous studies. The size and thickness of the debris-covered section of glacier was scaled according to the 2007 debris-covered/clean glacier area ratio. This means that although smaller in size, the debris-covered zones see an increase in the degree-day factor because of decreased thicknesses of sediment. Consequently, the 25%, 50%, and 75% glacier recessions see decreases in discharge of 23.6%, 45.0%, and 68.2% respectively (Table 4.7), yielding an average decrease of 0.92% total discharge per 1% shrinkage in glacier area. These decreases in discharge become smaller toward the end of the water year (Figure 4.14).

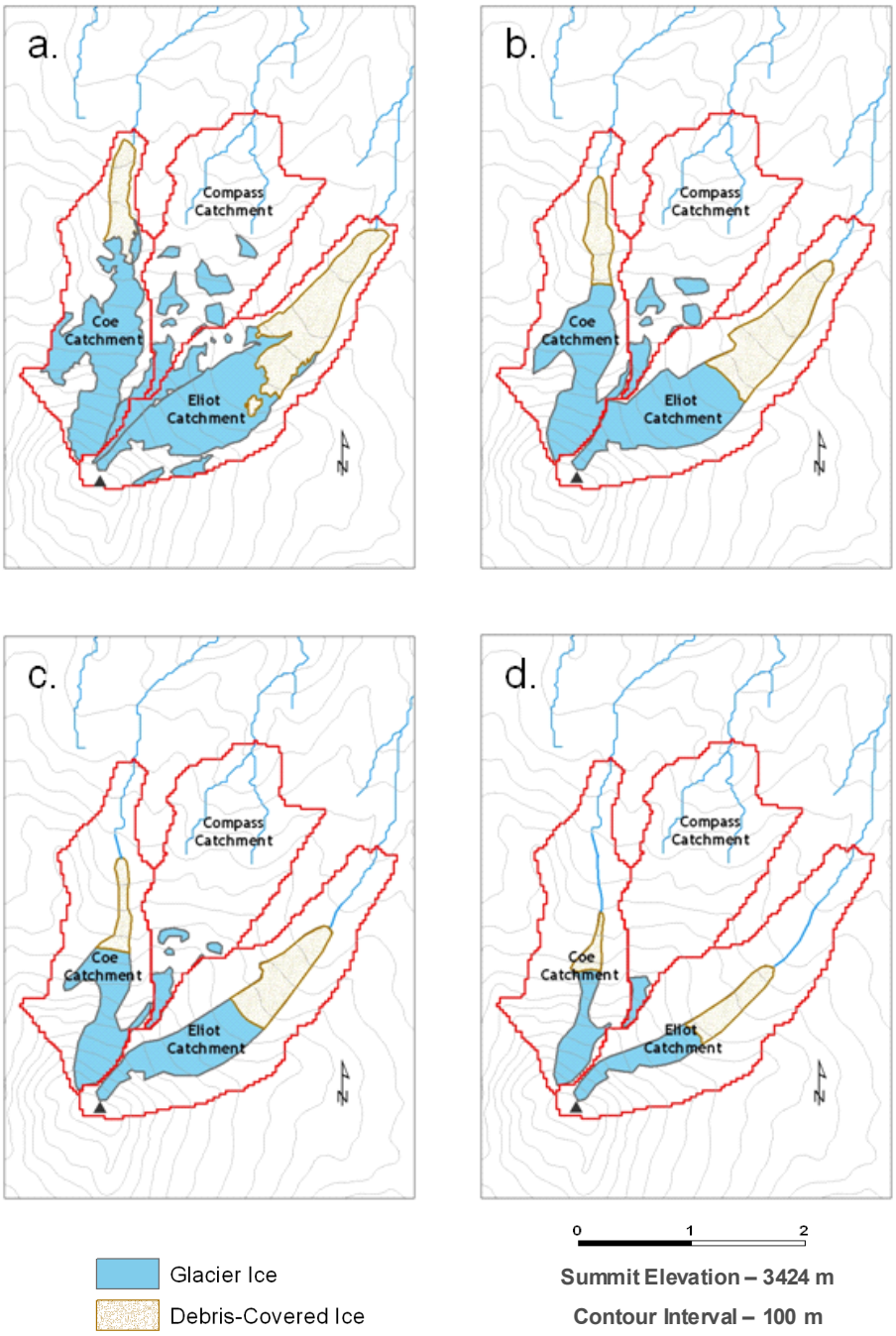

Figure 4.13 Glacier-covered areas in SRM recession simulations: a – 2007 glacier area, b – 25% recession, c – 50% recession, and d – 75% recession. Areas were delineated in ArcGIS and geometrically scaled according to historical retreat records.

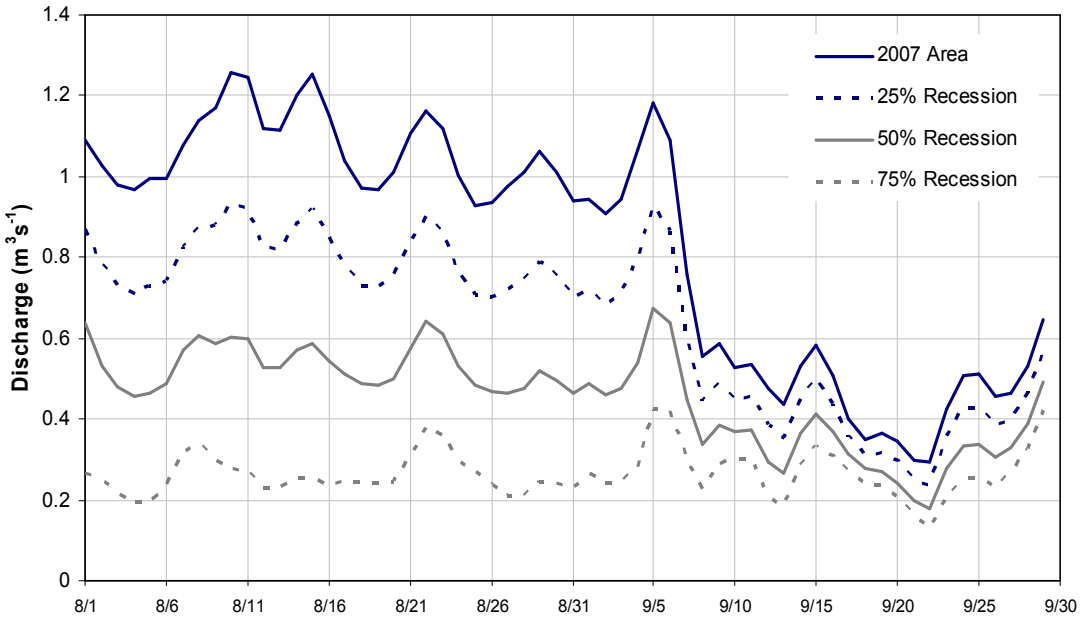

Figure 4.14 SRM glacier melt runoff sensitivity to glacier recession in the Eliot, Coe, and Compass Catchments.

Table 4.7 Total glacier discharge under different glacier area scenarios. Temperature is based on 25-year daily means, and precipitation was held constant at 0.

Glacier Cover	Total Discharge- 8/1-9/29 (m^3)	Change in Discharge from 2007 (%)
2007 Area	2.29×10^6	-
25% Recession	1.75×10^6	-23.6
50% Recession	1.26×10^6	-45.0
75% Recession	7.28×10^5	-68.2

4.39 *2059 Scenario*

To estimate the timing of future glacier retreat for the entire catchment, recent rates of retreat based on known locations of past glacier termini were extrapolated to future scenarios. The rate of retreat was calculated for the Eliot Glacier based on 2007 GPS coordinates and a 1989 recording (Lundstrom et al., 1993) of the glacier terminus. With a total recession of 284 m (Figure 4.15), the

Eliot Glacier has retreated at a rate of 15.8 m/year in the 18-year period. The extrapolation of this rate of retreat is likely a conservative measure because 1) the retreat has been accelerating over the last 50 years, and 2) changes in Eliot Glacier area have been shown to lag precipitation and temperature changes by 10-15 years (Jackson, 2007). The later factor implies that the glaciers do not yet reflect the recent warming period, whereby 11 of the 12 years prior to 2007 were the warmest on the instrumental record (IPCC, 2007b). Thus the retreat rate of Mount Hood glaciers is likely to accelerate in the near future. Interestingly, it was estimated that the glacier receded 25 m during the 2007 ablation season fieldwork.

Figure 4.15 The recession of the Eliot Glacier terminus from 1989-2007 shows a rate of retreat of 15.8 m/yr.

According to the aforementioned rate of retreat, the Eliot glacier will reach 50% of its size by approximately 2059. This glacier retreat rate was extrapolated to the Compass Catchment and reassigned a 50% GCA. Coe Glacier, which has retreated at a rate 27% slower than that of the Eliot in the last century (Jackson, 2007), was estimated to be 61% of its 2007 area in 2059. Since global temperatures are expected to increase by a range of 1.1 – 6.4°C in the next 100 years (IPCC, 2007), a reasonable increase of 2°C was applied to the simulation. Under this scenario (Figure 4.16), the glaciers will discharge 31.3% less in 2059 than the 2007

computation during the August-September time period (Table 4.8). August would see the greatest shortages, with a 37.5% total decrease. In contrast, the last few weeks of the water year see minimal changes; from 9/10 to 9/29, there is only a 10.8% decline in total runoff.

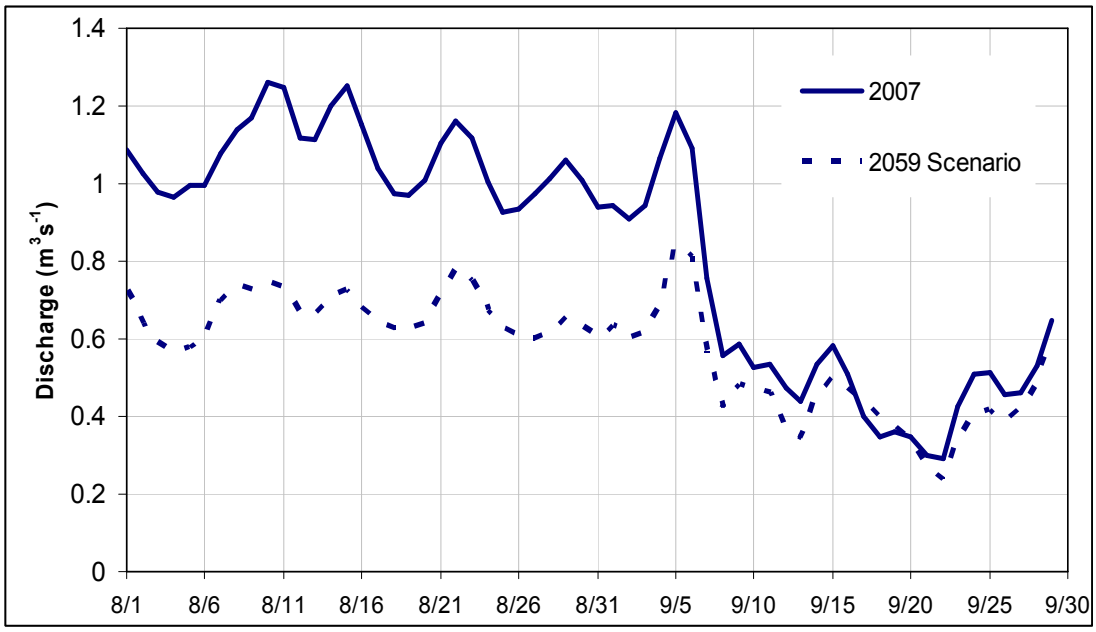

Figure 4.16 SRM simulations for 2007 GCA and 2059 GCA (estimated) under a 2°C forcing. 25-year mean temperatures are applied as baseline inputs and precipitation is set to 0 to isolate glacier melt.

Table 4.8 SRM simulations for 2007 GCA and 2059 GCA (estimated) under a 2°C forcing.

Scenario	Total Glacier Discharge (m^3)	Decrease in Discharge (%)
2007 Conditions	**4.34×10^6 m^3**	-
• August	2.85×10^6 m^3	-
• September	1.49×10^6 m^3	-
• 9/10-9/29	7.94×10^5 m^3	
2059 Conditions	**2.98×10^6 m^3**	**31.3**
• August	1.78×10^6 m^3	**37.5**
• September	1.20×10^6 m^3	**19.5**
• 9/10-9/29	7.08×10^5 m^3	**10.8**

Chapter 5: Discussion

5.1 Discharge and Stable Isotope Analyses

The application of stable isotope tracers and discharge measurements show that late summer 2007 flows in the Eliot and Coe Creeks are dominated by glacier meltwater. Because the Upper Middle Fork has been shown to be so dependent on glacier melt, the overall flow of the catchment is very sensitive to changes in temperature during the dry season, and less dependent on summer precipitation events. The findings of this study indicate that the disappearance of Mount Hood's glaciers will likely result in the loss of 41 – 74% of the overall discharge in the Upper Middle Fork at the end of the water year.

Quantifying catchment contributions based on the results from just one ablation season is not ideal, and ongoing discharge recordings are recommended for water planning of the Middle Fork. However it is worth noting that the field season in this study had similar weather characteristics to the long-term averages. August-September (2007) temperatures averaged to 10.4°C, whereas a 25-year mean is 11.3°C. Precipitation during this period totaled to 13.0 cm compared to a 27-year mean of 13.6 cm.

Measuring discharge in a dynamic environment such as this catchment comes with a host of potential errors. Turbulence can alter the flow signal and will misrepresent velocity on the flow meters. As mentioned earlier, sediment build-up at the base of the water recorders was also a problem. To compensate for the consequent discrepancy among height measurements, it was assumed that the rate of deposition was linear. This assumption is unrealistic. Finally, the Coe Glacier site

was observed to become more braided and to shift over time. This has consequences for the accuracy of a rating curve and could be the reason for questionable r^2 values (Appendix A).

Glacier meltwater was measured to be lighter (more depleted in ^{18}O) than the spring-fed streams down-catchment. This is likely because of the elevation effect on stable isotope composition. As air masses rise over mountains, adiabatic cooling leads to increased precipitation and progressive depletion of heavy isotopes. This depletion is enhanced at cooler temperatures, which allow for greater fractionation between liquid and vapor phases (Ingraham, 1998). This depletion rate has been measured to be a 3.2 ‰ decrease in $\delta^{18}O$ per 1000 meter increase in elevation (Siegenthaler and Oeschger, 1980). In this study, glacier samples exhibited a 3.2 ‰ decrease in $\delta^{18}O$ from the streams approximately 900 meters down-catchment, a rate similar to that of the aforementioned study. Additionally, since the springs are lower in elevation and are likely recharged by rainfall, it is not surprising that they are less depleted in ^{18}O than the glacier-fed systems. According to Clark and Fritz (1997), in catchments where there is pronounced seasonalilty, rain is frequently isotopically heavier than snow fall. There is a surprisingly significant difference between the ^{18}O composition of glacier meltwater (-13.35‰) and that of glacier ice (-14.34‰), even for the ice that was sampled just meters away from the outlet stream.

It is important to note that there were several assumptions made in the derivation of glacier melt from ^{18}O tracers, as noted by other ^{18}O analyses (Sklash and Farvolden, 1979):

- The ^{18}O content of the glacier meltwater (event water) is significantly different from the spring water (pre-event water).

- The glacier meltwater component of runoff was constant between the time of meltwater sampling and downstream sampling.
- There is minimal surface storage contribution to runoff.
- Vadose water contributions to runoff are negligible.

There are other assumptions, unique to this study, which contribute to error in the estimation of glacier melt content in the downstream sites. It was assumed that the ^{18}O content was consistent among all glaciers and glacierettes in a given catchment. This assumption is not problematic in the Eliot catchment for there is only one outlet stream at the tongue of the Eliot Glacier. However the Coe catchment has several streams that originate from sources other than the sampled Coe Glacier. These sources include isolated glacierettes, permanent snowfields, and remnants of the Langille Glacier. If these streams are more depleted in ^{18}O than the upper Coe Creek, then the mixing model would have overestimated the total glacier contributions. For example, if the streams actually had an ^{18}O content of -13.2‰ (versus assuming the same content as Coe Glacier: -12.82‰) during first collection period, then the actual meltwater contributions would have been 14% less than what was reported.

This study could be further improved by an increased sample size. With only 24 isotope samples collected for analysis, there was no room for a true hydrograph separation. In situ use of a laser spectrometer would be ideal in this setting.

5.3 Glacier Runoff Modeling

Glacier retreat and temperature increases influence glacier runoff in opposite manners; a decrease in GCA yields lower discharges whereas an increase in temperatures during the ablation season promotes greater runoff. The relative importance of each factor determines whether or not glacier runoff increases or decreases in the future. As stated earlier, the SRM simulations (8/1-9/29) show that the Eliot Glacier discharge increases 13.8% for every 1°C increase, but lowers 9.2% for every 10% decrease in glacier area. Thus, for runoff to be in equilibrium over time the glacier must shrink by 15% at the same rate that temperatures will increase by 1°C. The retreat of the Eliot Glacier in the last century already exceeds this rate; therefore its discharge has likely been decreasing over time and will continue to decrease.

Eliot and Coe Glaciers have been shown to have major zones of debris cover, which are overlooked by the standard USGS quads (Figure 4.6). This study emphasizes the importance of debris-cover in determining the glacier's overall degree-day factor and its consequent runoff. In fact, the Eliot Glacier, with 41.6% of its area covered in sediment, is hydrologically equivalent to a clean glacier that is just 79% of its size. It is therefore important that future glacier melt studies use field observations, aerial photography, and/or advanced remote sensing techniques (Taschner and Ranzi, 2002; Frank et al., 2004) to precisely separate clean ice from debris-covered ice. Similar to other areas, Mount Hood has seen many studies documenting the retreat of its glaciers (Lillquist and Walker, 2006; Dodge, 1987; Driedger and Kennard, 1986), but little is known about the history or fate of the

debris-covered zones. In this study, the retreat rate in debris cover was assumed to be proportional to the documented retreat rate of the overall glaciers. However, the validity of this assumption is uncertain. In conclusion, in order to accurately forecast future glacier melt, there needs to be a greater understanding of the retreat of the clean ice/debris-cover boundary.

It is important to note that the use of SRM in this environment has several vulnerabilities to error. SRM was calibrated with discharge measurements taken at a stream with high turbulence and sediment fluxes. The normalizing of weather conditions on the glacier required long term averages to be applied to the SRM. However according to Braun et al. (2000) calculating mean daily precipitation and temperature values in a catchment filters out true weather patterns and makes the model less precise.

A lack of historical discharge records also contributed to error in the model simulations. With no streamflow records, it was necessary to generate runoff and recession coefficients in the calibration process. Runoff coefficients for both rain and snow vary throughout the water year (Guo, 2007), and these parameter changes were applied to match the decreasing runoff volumes over the two-month period (Appendix E). Because values for the degree-day factors in each glacier zone were held constant, changes in the runoff coefficients may have been overemphasized.

One difficulty of using a temperature-index model such as the SRM is that it is hard to accurately model the spatial variability in melt due to local differences in slope, aspect, and shading (Hock, 2003). Properly calculating spatial variability is important in a study such as this one because as glaciers retreat they often become

more shaded, and overall melting decreases. This is a shortcoming of this study's approach, and as a result the effect of glacier recession on glacier melt might be underestimated. A future study could incorporate solar radiation reception into SRM as performed by Brubaker et al. (1996), but this would require the installation of a more sophisticated weather station on Mount Hood.

As modeling techniques and data acquisition become more sophisticated, there has been a push to not only validate the models precisely, but also to validate the models for the right reasons (McDonnell et al., 2007). In other words, modelers are arguing to focus more on input accuracy and less on input calibration. Striving for such a goal becomes a problem in basins with few meteorological and hydrological records. By calibrating the runoff coefficients to measured discharge in this study, the model could be reasonably validated, but there exists uncertainty about parameter accuracy, particularly for runoff coefficients and the degree-day factor. In the model, the adjustment of the runoff coefficient provided for intense decline in discharge in September. Runoff may rapidly decrease in September for a variety of other reasons, related to decreased temperature, the depletion of englacial, subglacial, firn storage late in the ablation season (Seaberg et al., 1988; Hock and Hooke, 1993), and the decreasing solar reception during this period. A future study could better capture the temporal variability of the degree-day factor by experimentally measuring ablation each day in both the ablation and accumulation zones. In the end though, the simulation output would be the same because the degree-day factor has the same weight as the runoff coefficient in the calculation of runoff (Equation 1.2) when precipitation is negligible.

Chapter 6: Conclusion

In the age of advanced hydrologic modeling and measuring techniques, the question still remains of how best to measure and predict glacier runoff in small, ungauged catchments. These catchments have frequently been overlooked because inaccessibility, harsh conditions, and a consequent void of discharge records. Furthermore, many of the snow and glacier melt models have evolved to focus on larger basins, where discharge records are available for calibration and remote sensing can reasonably estimate changes in snow-covered area. These studies typically use Moderate Resolution (MODIS) images, which have good temporal resolution, and a spatial resolution that is appropriate to the basin scale. This approach however is not transferrable to smaller catchments, which require higher-resolution data and often lack discharge records. This paper therefore proposes a method for quantifying present and future glacier melt contributions in catchments that have been inadequately modeled.

Despite the aforementioned difficulties and errors associated with measuring discharge in glacierized basins, the importance of glaciers to the Middle Fork Hood River is undeniable. Between 8/10/2007 and 9/7/2007, the glacier-fed Eliot and Coe Creeks contributed 76% of the total flow to this catchment. 76 – 88% of Eliot Creek's discharge was calculated to be glacier melt at this time. In total, the Coe and Eliot Glaciers contributed 41 – 74% of the surface runoff in the Upper Middle Fork Catchment.

According to SRM simulations discussed in this paper, the Upper Middle Fork catchment of the Hood River, Oregon exhibits high sensitivity to changes in the

area, debris-cover, and air temperatures of the Eliot, Coe, and Compass glaciers and glacierettes. Validation of the SRM parameters met a reasonable Nash-Sutcliffe coefficient of 0.81 when applied to the Coe Glacier. Using glacier recession rates and established temperature increases, the model indicates a decrease in total glacier discharge of 31.3% by the year 2059. In this and other scenarios, August undergoes particularly drastic changes in discharge, whereas the period from early September to the end of the water year sees much smaller losses, probably because of the decreased degree-day factor and increases in precipitation inputs at this time.

These findings should be considered in the water planning of the Middle Fork Irrigation District. Glaciers have been demonstrated to play a key role in water supply to their diversion systems in August and September, a time of severe low flows, and a time when water is needed for the harvesting fruit orchards. Glacier recession points toward the increased severity of these low flows, especially during the month of August.

The methods provided in the paper serve as a strategy for gauging glacier runoff in the late ablation season in small, ungauged catchments. Calibration of the SRM requires a minimum of one season of ongoing discharge measurements; however a longer record of discharge would enable better approximation of runoff and recession coefficients, as well as a separate year for validation. Runoff simulations can be normalized by long-term precipitation records. Late season ASTER data coupled with aerial photographs and GPS waypoints can determine the glacier-covered area of the catchment, and can be considered a constant SRM input at the end of the ablation season. By subtracting precipitation and groundwater

inputs from the model, one can calculate future glacier runoff in response to glacier recession and increased temperatures.

Future research in the Hood River Basin can focus on the impact of glacier recession on stream and mainstem temperatures. Temperature increases may deter the spawning of already-threatened fish. For instance the Bull Trout, an anadromous fish that regularly spawns in the Upper Middle Fork, was listed in 1998 as a "threatened species" under the Federal Endangered Species Act. It is particularly sensitive to temperatures greater than 10°C. However recent surveys have indicated that the maximum allowable temperature of 12°C has been exceeded within the catchment (Hood River Local Advisory Committee, 2004). The basin may also benefit from an assessment of the economic impact of glacier recession, one that combines the effects on water supply, hydropower, and tourism, as has been done recently in other mountainous regions (Vergara et al., 2007).

Bibliography

Abal'yan, T.S., V.M. Mukhin, and Y.A. Polunin, On glacial nourishment and possibilities of long-term prediction of the mountain river's runoff with vast glacierization of the catchment areas. *The Data of Glaciological Studies*, 39, 42–49, 1980.

Anderson, E.A., National weather service river forecast system—snow accumulation and ablation model. NOAA Technical Memo, NWS HYDRO-17, US Dept. Commerce, Washington, DC, USA 1973.

Baker, D., H. Escher-Vetter, H. Moser, and O. Reinwarth, A glacier discharge model based on results from field studies of energy balance, water storage and flow, *Proceedings of the Hydrological Aspects of Alpine and High Mountain Areas, Exeter Symposium, IAHS pub. No. 138*, 103-112, 1982.

Barry, R.G., *Mountain weather and climate* (2nd ed.), Routledge, London, England, 1996.

Borovikova, L.N., Y.M. Denisov, F.B. Trofimova, and I.D. Shentsis, On mathematical modelling of the mountain rivers' runoff, *Matematicheskoye modelirovanie protsessa stoka gornukh rek*, Hydrometeoizdat, 152, 1972.

Braithwaite, R.J., Positive degree–day factors for ablation on the Greenland ice sheet studied by energy-balance modelling. *Journal of* Glaciology, 41, 153–160, 1995.

Braithwaite, R.J., Air temperature and glacier ablation—a parametric approach. PhD Thesis, McGill University, Montreal, Canada, 1977.

Braithwaite, R.J., On glacier energy balance, ablation and air temperature, *Journal of Glaciology,* 27, 381–391, 1981.

Braithwaite, R.J. and O.B. Olesen, Winter accumulation reduces summer ablation on Nordbogletscher, South Greenland, *Zeitschrift für Gletscherkunde und Glazialgeologie.* 24, 21–30, 1988.

Braun, L.N., M. Weber, M. Schulz, Consequences of climate change for runoff from Alpine regions, *Annals of Glaciology*, 31, 19–25, 2000.

Brubaker, K., A. Rango, and W. Kustas, Incorporating radiation inputs into the snowmelt runoff model, *Hydrological Processes*, 10, 1329-1343, 1996.

Cameron, K.A. and P.T. Pringle, A detailed chronology of the most recent major eruptive period at Mount Hood, Oregon, *Geological Society of America Bulletin 99*: 845-851, 1987.

Chennault, J., 2004, Modeling the contributions of glacial meltwater to streamflow in Thunder Creek, North Cascades National Park, Washington. Master's Thesis, Western Washington University, Bellingham, Washington, 88 p., 2004.

Clark, I. and P. Fritz, Environmental Isotopes in Hydrogeology, Lewis, Boca Raton, Florida, 1997.

Craig, H., Isotope variations in meteoric waters, *Science*, 133, 1702-1703, 1961.

Dincer, T., B.R. Payne, T. Florkowski, J. Martinec, and E. Tongiorgi, Snowmelt runoff from measurements of tritium and oxygen-18, *Water Resources Research*, 34, 915-919.

Dodge, N.A., Eliot Glacier: net mass balance, *Mazama*, 69(13), 52-55, 1987.

Donnell, C.B., Quantifying the glacial meltwater component of streamflow in the Middle Fork Nooksack River, Whatcom County, WA using a distributed hydrology model, Master's Thesis, Western Washington University, Bellingham, Washington, 103 p., 2007.

Driedger, C and P. Kennard, Ice Volumes on Cascade Volcanoes-Mount Rainier, Mount Hood, Three Sisters, and Mount Shasta, *U.S. Geological Survey Professional Paper 13826*, 28 p, 1986.

Earman, S., A.R. Campbell, F.M Phillips, and B.D. Newman, Isotopic exchange between snow and atmospheric water vapor: Estimation of the snowmelt component of the groundwater recharge in the southwestern United States, *Journal of Geophysical Research*, 111, 2006.

Escher-Velter, H. The radiation balance of Vernagtferner as a basis of the energy budget computations for the determination of the melt water production of an Alpine glacier, Wiss. Mitt. Inst. 39, 1980.

Escher-Vetter, H., Energy balance calculations for the ablation period 1982 at Vernagtferner, Oetztal Alps. *Annals of Glaciology* 6, 158–60, 1985.

Ferguson, R.I., Snowmelt Runoff Models, Progress in Physical Geography, Vol. 23, (2), 205-227, 1999.

Fountain, A.G., The storage of water in, and hydraulic characteristics of, the firn of South Cascade Glacier, Washington State, USA. *Annals of Glaciology*, 13, 69–75, 1989.

Fountain, A.G., Effect of snow and firn hydrology on the physical and chemical characteristics of glacial runoff. *Hydrological Processes*, 10(4), 509–521, 1996.

Fountain, A.G., and W.V. Tangborn, The effect of glaciers on streamflow variations, *Water Resources Research*, 21(4), 579–586, 1985.

Fountain, A.G., and J.S. Walder, Water flow through temperate glaciers. *Review of Geophysics*, 36(3), 299–328, 1998.

Fountain, A.G., and W.V. Tangborn, The effect of glaciers on streamflow variations, *Water Resources Research*, 21(4), 579-586, 1985.

Frank P., C. Huggel, and A. Kaab, Combining satellite multispectral image data and a digital elevation model for mapping debris-covered glaciers, *Remote Sensing of the Environment,* 89(4), 510-518, 2004.

Glaciers of the American West. Data provided by Portland State University, Departments of Geography and Geology, <http://glaciers.research.pdx.edu>, Accessed 2007 Oct 14.

Golubev, G.N., Analysis of the runoff and flow routing for a mountain glacier basin, *IAHS Publication No. 95*, 41-50, 1973.

Guo, H., B. Su, Y. Wang, T. Jiang, Runoff coefficients change and the analysis of the relationship between climate factors and runoff coefficients in Poyang Lake Basin (China), 1955-2002, *Journal of Lake Sciences*, 19(2), 163-169, 2007.

Hastenrath, S. and A. Ames, Diagnosing the imbalance of Yanamarey Glacier in the Cordillera Blanca of Peru, *Journal of Geophysical Research*, 100(D3), 5105-5112, 1995.

Hochstein**,** M.P., D. Claridge, S.A. Henrys, A. Pyne, D.C. Nobes, D.C. and S. Leary, Downwasting of the Tasman Glacier, South Island, New Zealand: changes in the terminus region between 1971 and 1993. *New Zealand Journal of Geology and Geophysics*, 38, 1–16, 1995.

Hope, G., J. Pask, Z. Li, W. Sun, and Q. Zeng, Measurements of glacier variation in the Tibetan Plateau using Landsat data, *Remote Sensing of the Environment*, 63(3), 258-264, 1998.

Hock, R., Glacier melt: a review of processes and their modeling, *Progress in Physical Geography*, 29(3), 362-391, 2005.

Hock, R., Temperature index melt modeling in mountain areas, Journal of Hydrology, 282(1-4), 104-115, 2003.

Hock, R., and R. Hooke, Evolution of the internal drainage system in the lower part of the ablation area of Storglaciaren,Sweden. *GSA Bulletin No. 105* (4), 537–546, 1993.

Hood River County, Basic County Information, http://www.co.hood-river.or.us/, 2003, Accessed 2008 May 15.

Hood River Local Advisory Committee, Hood River Agricultural Water Quality Management Area Plan (2nd Biennial Revision), Nov. 18, 2004.

Ingraham, N.L, Isotopic variations in precipitation, In: Isotope Tracers in Catchment Hydrology, [eds. C. Kendall and J.J. McDonnell], Elsevier Publishing, Amsterdam, The Netherlands, 87-118, 1998.

International Panel on Climate Change (IPCC) Climate Change 2007: *Impacts, Adaption and Vulnerability, Contribution of Working Group II to the Third Assessment Report of the Intergovernmental Panel on Climate Change*, [eds. J.J. McCarthey et al.], Cambridge Univ. Press, New York, 2007a.

International Panel on Climate Change, IPCC, Climate Change 2007: The Physical Science Basis. Contribution of Working Group I to the Fourth Assessment Report of the Intergovernmental Panel on Climate Change, [eds. S. Solomon et al.], Cambridge University Press, 2007b.

Jackson , K.M., and A.G. Fountain, Spatial and morphological change on Eliot Glacier, Mount Hood, Oregon, USA, *Annals of Glaciology*, 46**,** 2007.

Jackson, K. M., Spatial and Morphological Change of Eliot Glacier, Mount Hood, Oregon, Ph.D. dissertation, Portland State University, Portland, Oregon, 111 p, 2007.

Jansson, P., R. Hock, and P. Schneider, The concept of glacier storage: a review, *Journal of Hydrology*, 282, 116-129, 2003.

Johannesson, T., O. Sigurosson, T. Laumann, and M. Kennett, Degree–day glacier mass balance modelling with applications to glacier in Iceland, Norway and Greenland, *Journal of Glaciology,* 41, 345–358, 1995

Kaab, A., F. Paul, C. Huggel, H. Kieffer, J. Kargel, and R. Wessels. Glacier monitoring from ASTER imagery: accuracy and applications*, EARSeL eProceedings, Observing our Cryosphere from Space*, 43-53, 2002.

Kasser, P., Der Einfluss von Gletscherrückgang und Gletschervorstoss auf den Wasserhaushalt. *Wasser- und Energiewirschaft*, 51, pp. 155–168, 1959.

Kayastha, R.B., Y. Takeuchi, M. Nakawo, and Y. Ageta, Practical prediction of ice melting beneath various thickness of debris cover on Khumbu Glacier, Nepal, using a positive degree-day factor, *Debris-Covered Glaciers, IAHS Publication no. 264*, 71-81, 2000.

Krimmel, R.M., and W.V.Tangborn, South Cascade Glacier: The moderating effect of glaciers on runoff, paper presented at the Western Snow Conference, Anchorage, Alaska, 1974.

Kuhn, M. Methods of assessing the effects of climatic changes on snow and glacier hydrology. *Snow and glacier hydrology. Proceedings of the Kathmandu Symposium 1992: IAHS Publ. no. 218*,135–144, 1993.

Kustas, W.P., A. Rango, and R. Uijlenhoet, A simple energy budget algorithm for the snowmelt runoff model, *Water Resources Research*, 30(5), 1515-1527, 1994.

Lang, H., Forecasting meltwater runoff from snow-covered areas and from glacier basins., In: River Flow Modeling and Forecasting, Kraijenhoff, [eds. D.A., Moll, J.R. Reidel], Dordrecht, The Netherlands, 99–127, 1987.

Lang, H., Schädler, B. and Davidson, G., Hydroglaciological investigations on the Ewigschneefeld-Gr. Aletschgletscher, *Zeitschrift für Gletscherkunde und Glazialgeologie* 12, 109–124, 1977.

Laumann, T. and Reeh, N., Sensitivity to climate change of the mass balance of glaciers in southern Norway. *Journal of Glaciology,* 39, 656–665, 1993.

Lillquist K., and K. Walker, Historical glacier and climate fluctuations at Mount Hood, Oregon, *Arctic, Antarctic, and Alpine Research*, 38(3), 399-412, 2006.

Lundquist, D., Modeling Runoff from a Glacierized Basin, *Hydrological Aspects of Alpine and High-Mountain Areas IAHS Publication No. 138*, 131-136, 1982.

Lundstrom, S.C., The budget and effect of superglacial debris on Eliot Glacier, Mt. Hood, Oregon. Ph.D. dissertation, University of Colorado, Boulder, Colorado, 183 p., 1992.

Lundstrom, S.C., A.E. McCafferty, J.A. and Coe, Photogrammetric analysis of 1984-1989 surface altitude change of the partially debris-covered Eliot Glacier, Mt. Hood, Oregon, U.S.A., *Annals of Glaciology*, 17, 167-170, 1993.

Male, D.H. and R.J. Granger, Snow surface energy exchange, *Water Resources Research*, 17, 609-627, 1981.

Mark, B. G., and Seltzer, G. O., Tropical Glacier Meltwater Contribution to Stream Discharge: A Case Study in the Cordillera Blanca, Peru, *Journal of Glaciology*, 49 (165), 2003.

Marks, D. and J. Dozier, Climate and Energy Exchange at the Snow Surface in the Alpine Region of the Sierra Nevada: Snow Cover Energy Balance, *Water Resources Research*, 28(11), 3043-3054, 1992.

Martinec, J. (1975). New methods in snowmelt-runoff studies in representative basins. *IAHS Symposium on Hydrological Characteristics of River Basins, Tokyo, Japan*, 117, 99-107, 1975 .

Martinec, J., A. Rango, and R. Roberts, Snowmelt Runoff Model (SRM) User's Manual, Updated Edition for Windows (WinSRM Version 1.11), 2007.

Martinec, J., and A. Rango, Merits of statistical criteria for the performance of hydrological models, *Water Resources Bulletin* 25(2), 421-432, 1989.

Martinec, J., and A. Rango, Parameter Values for Snowmelt Runoff Modelling, *Journal of Hydrology*, 84 (3), 197-219, 1986.

Martinec, J. The degree-day factor for snowmelt runoff forecasting. In *IUGG General Assembly of Hel-sinki, IAHS Commission of Surface Waters*, *IAHS publ. no. 51*, 468–477, 1960.

Mayo, L.R, Glacier Mass Balance and Runoff Research, *Geografiska Annaler*, in the U. S. A., 66(3), 215-227, 1984.

McDonnell, J.J., M. Sivapalan, K. Vache,S. Dunn, G. Grant, R. Haggerty, C. Hinz, R. Hooper, J. Kirchner, M. L. Roderick, J. Selker, and M. Weiler, Moving beyond heterogeneity and process complexity: A new vision for watershed hydrology, *Water Resources Research*, 43, 2007.

Milstein, M. "When Glaciers Melt", *The Oregonian*, March 26, 2006.

NASA Jet Propulsion Laboratory: ASTER., 2004 Sept 7, <http://asterweb.jpl.nasa.gov/>, Accesed 2007 Oct 21.

Nash, J. E. and J. V. Sutcliffe (1970), River flow forecasting through conceptual models part I—A discussion of principles, *Journal of Hydrology*, 10(3) ,282 290.

National Agricultural Imagery Program, 2006 Information Sheet. <http://165.221.201.14/NAIP.html>, Accessed 2008 May 5.

Obradovic, M.M., and Sklash, M. G., An Isotopic and Geochemical Study of the Snowmelt Runoff in a Small Arctic Watershed, *Hydrological Processes*, 1, 15-30, 1986.

Ohmura, A. Physical basis for the temperature-based melt-index method. *Journal of Applied Meteorology,* 40, 753–761, 2001.

Orheim, O., Glaciological investigations of Store Supphellebre, West-Norway, Norway Polar Institute, Norway, 151 p., 1970.

Power, J.M, and G.J. Young, Application of an operational hydrologic forecasting model to a glacierized research basin, *Proceedings of the Third Northern Research Basin Symposium Workshop, Quebec City,* 1979.

Quick, M.C. and A. Pipes, U.B.C. Watershed Model, *Hydrological Sciences Bulletin*, 22(1), 153-161, 1977.

Rango, A. and J. Martinec, Revisiting the degree-day method for snowmelt computation. *Water Resources Bulletin*, 31(4), 657-669, 1995.

Rodhe, A., Springflood – Meltwater or Groundwater? *Nordic Hydrology*, 12(1), 21-30, 1981.

Salomonson, V.V., W.L. Barnes, P.W. Maymon, H.E. Montgomery, and H. Ostrow, MODIS: advanced facility instrument for studies of the Earth as a system, *Geoscience and Remote Sensing*, 27(2), 145-153, 1989.

Schaper, J. and K. Seidel, Modeling Daily Runoff from Snow and Glacier Melt Using Remote Sensing Data, *Proceedings of EARSeL-SIG-Workshop Land Ice and Snow, Dresden, No. 1*, 308, 2000.

Schneider, T., Hydrological processes in the wet-snow zone of glacier: a review. *Z.* Gletscherkd. Glazialgeol. 36(1), 89–105, 2000.

Schytt, V., Scientific results of the Swedish glaciological expedition to Nordaustlandet Spitsbergen, 1957 and 1958, *Geografiska Annaler,* 46(3), 243–281, 1964

Seaberg, S.Z., J.Z. Seaberg, R.L.Hooke, and D.W. Wiberg, Character of the englacial and subglacial drainage system in the lower part of the ablation area of Storglacia¨ren, Sweden, as revealed by dye-trace studies, *Journal of Glaciology*, 34(117), 217–227, 1988.

Shanley, J.B., C. Kendall, M.R. Albert, J.P. Hardy, Chemical and isotopic evolution of a layered eastern U.S. snowpack and its relation to stream-water composition, *IAHS Publication No. 228*, 329-338, 1995.

Sherrod, D.R. and J.G. Smith, Quaternary extrusion rates of the Cascade Range, Northwestern United States and Southern British Columbia*, Journal of Geophysical Research*, 95(b12), 19465-19474, 1990.

Sidjack, R.W., and R.D. Wheate, Glacier mapping of the Illecillewaet icefield, British Columbia, Canada using Landsat TM and digital elevation data, International Journal of Remote Sensing, 20(2), 273-284, 1999.

Siegenthaler, U. and H. Oeschger, Correlation of ^{18}O in precipitation with temperature and altitude, *Nature*, 285, 314-317, 1980.

Singh, P., N. Kumar, and M. Arora, Degree-day factors for snow and ice for Dokriani Glacier, Garhwal Himalayas, Journal of Hydrology, 235, 2000.

Singh, P. and V. Singh, Snow and Glacier Hydrology, Kluwer Academic Publishers, Dordrecht, The Netherlands, 2001.

Singh, P. and Kumar, N., Determination of snowmelt factor in the Himalayan Region, *Hydrological Sciences,* 41, 301–310, 1996.

Songweon L., A.G. Klein, and T.M. Over, A comparison of MODIS and NOHRSC snow-cover products for simulating streamflow using the Snowmelt Runoff Model, *Hydrological Processes*, 19 (15), 2951-2972, 2005.

Sklash, M. G., and Farvolden, R. N., The Role of Groundwater in Storm Runoff, *Journal of Hydrology*, 43, 45-65, 1979.

Tangborn, W.V., R.M. Krimmel, M.F. Meier, A comparison of glacier mass balance by glacier hydrology and mapping methods, South Cascade Glacier, *Snow and Ice—Symposium—Neiges et Glaces. Proceedings of the Moscow Symposium, August 1971. IAHS Publication No. 104,* 185–196, 1975.

Taschner, S., and R. Ranzi, Comparing the opportunities of Landsat-TM and ASTER data for monitoring a debris covered glacier in the Italian Alps within the GLIMS project, *Geoscience and Remote Sensing Symposium, 2002, IEEE International***,** 2, 1044-1046, 2002.

Thompson, L. G., Ice Core Studies from Mt. Kenya, Africa, and their Relationship to other Tropical Ice Core Studies, *Proceedings of the Canberra Symposium, IAHS Publication N. 121*, 55-62, 1981.

Vergara, W., A. M. Deeb, A. M. Valencia, R. S. Bradley, B. Francou, A. Zarzar, A. Grünwaldt, and S. M. Haeussling , Economic Impacts of Rapid Glacier Retreat in the Andes, *Eos Transactions-American Geophysical Union*, 88(25), 261, 2007.

Walters, R.A., and M.F. Meier, Variability of glacier mass balances in western North America. In Peterson, D. H. (ed.) Aspects of Climate Variability in the Pacific and the Western Americas. Washington: American Geophysical Union, 365–374, 1989.

Ward, R.C. and M. Robinson. Principles of Hydrology, 3rd Ed., McGraw Hill, Maidenhead, U. K., 365 p., 1990.

Wigmosta, M.S., L.W. Vail, and D.P. Lettenmaier, A distributed hydrology vegetation model for complex terrain, *Water Resources Research*, 30(6), 1665-1679, 2004.

Willis, I.C., N.S. Arnold, and B.W. Brock, Effect of snowpack removal on energy balance, melt and runoff in a small supraglacial catchment. *Hydrological Processes*, 16, 2721–2749, 2002

Wise, Geology of the Mount Hood Volcano – Andesite Conference Guidebook: International Mantle Project, *Oregon Department of Geology and Mineral Industries Bulletin*, 62, 81-98, 1968.

Woo, M.K. and B.B. Fitzharris, Reconstruction of mass balance variations for Franz Josef Glacier New Zealand, 1913–1989. *Arctic and Alpine Research,* 24, 281–290, 1992.

WMO, Intercomparison of models of snowmelt runoff. *Operational Hydrology Report*, World Meteorological Organization (WMO), Geneva, Switzerland, 1986.

Yoshida, S., Hydrometeorological study on snowmelt. *Journal of Meteorological Research*, 14, 879–899, 1962.

Zhang, Y., L. Shiyin, and D. Yongjian, Observed degree-day factors and their spatial variation on glaciers in western China, *Annals of Glaciology*, 43, 301-306, 2006a.

Zhang, Y, S. Liu, C. Xie, Y. Ding, Application of a degree-day model for the determination of contributions to glacier meltwater and runoff near Keqicar Baqi glacier, southwestern Tien Shan, *Annals of Glaciology*, 43 (1), 280-284, 2006b.

Appendices

Appendix A. Rating curves for the glaciers and creeks of the Upper Middle Fork Catchment Hood River. Pinnacle Creek was measured at a relatively constant discharge during the study period and no rating curve was necessary.

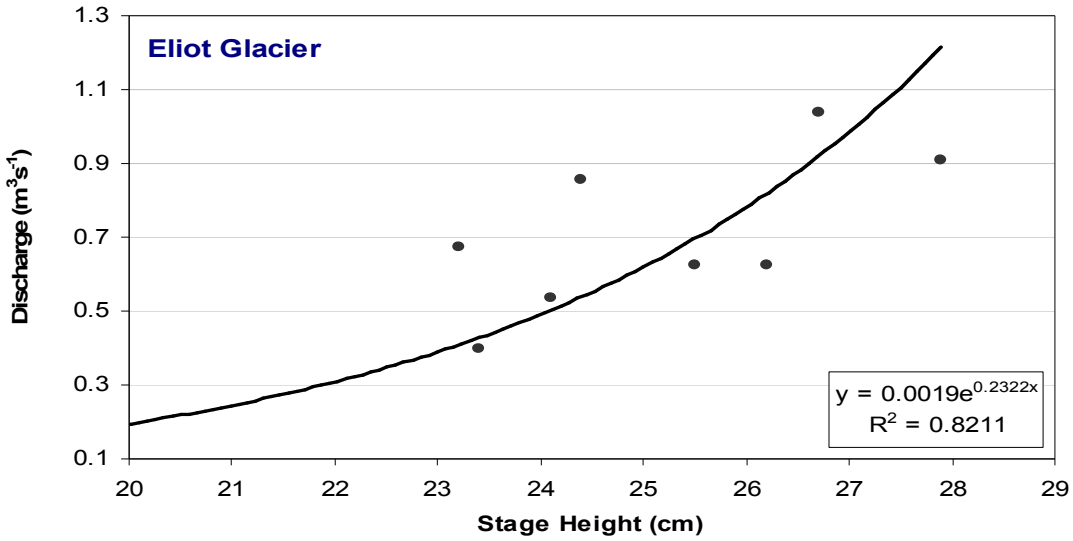

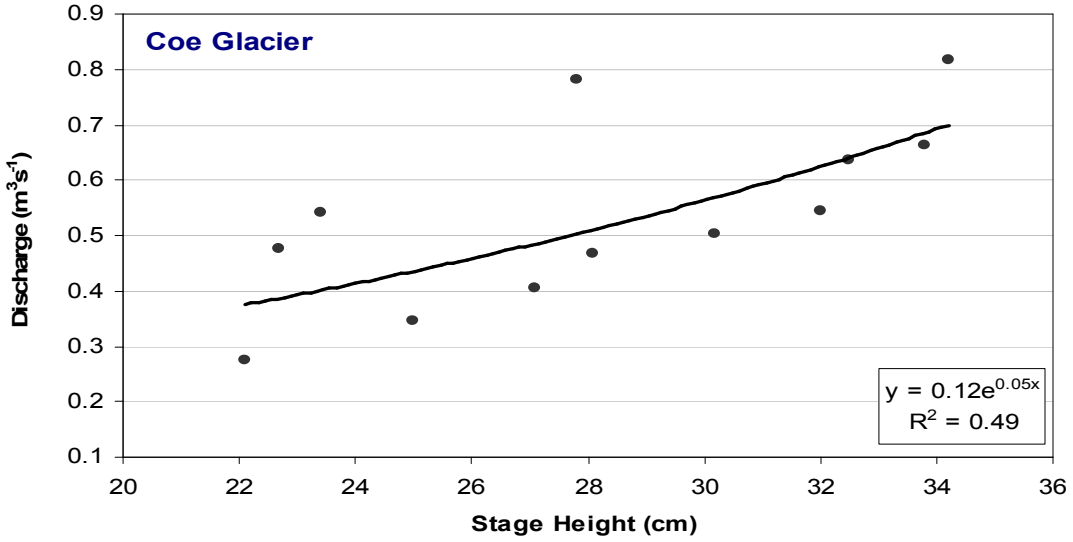

Appendix A (continued)

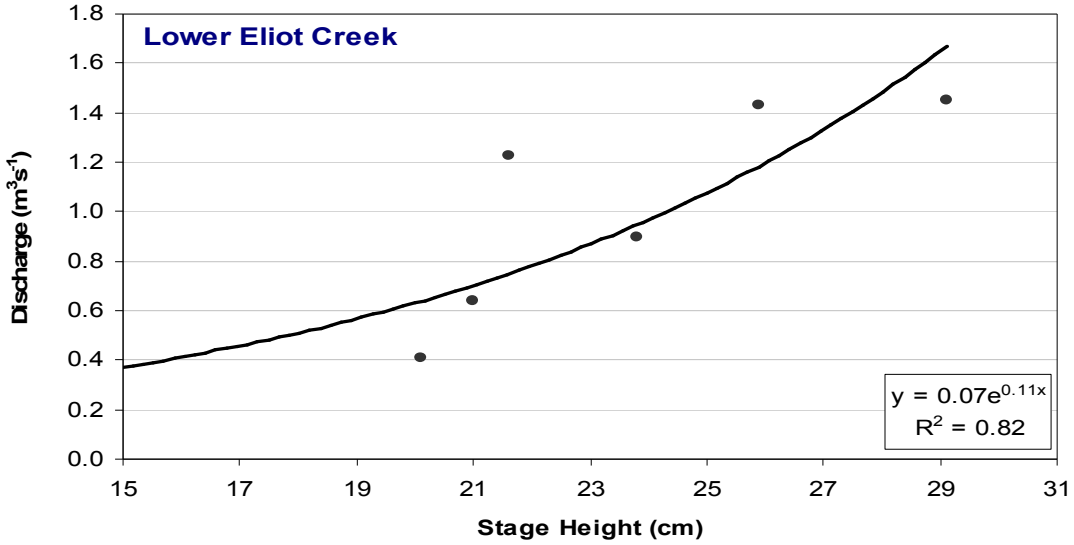

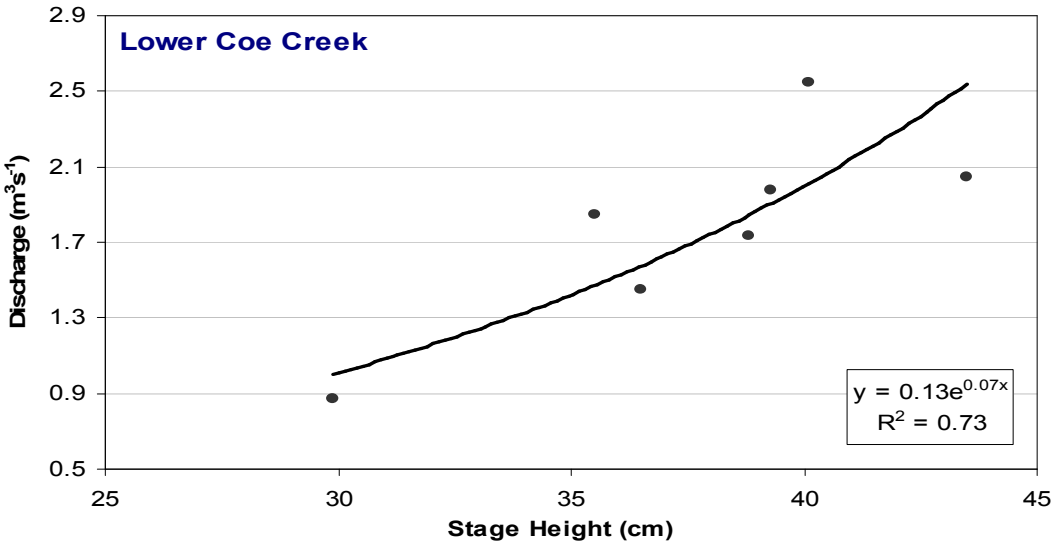

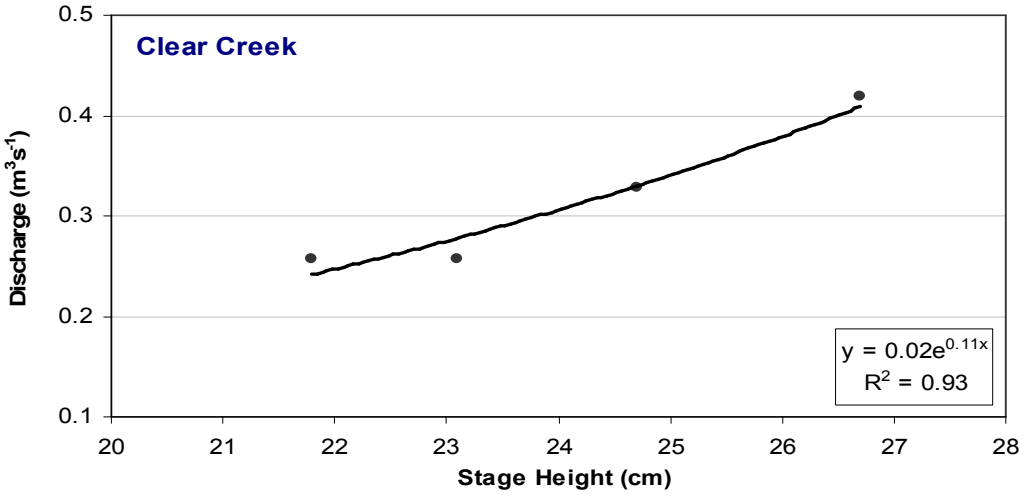

Appendix B. Steps required for a watershed delineation in ArcGIS. Ensure that ArcHydro™ tools are downloaded and use the Interactive Point Delineation tool.

1. DEM Reconditioning
2. Fill Sinks
3. Flow Direction
4. Flow Accumulation
5. Stream Definition
7. Catchment Grid Delineation
8. Catchment Polygon Processing
9. Drainage Line Processing
10. Adjoint Catchment Processing
11. Drainage Point Processing
12. Drainage Density Evaluation
13. Batch Watershed Delineation

Appendix C. Basin Setup for SRM using ArcGIS

1. Create or acquire shapefiles for all glaciers, debris-covered glaciers, and glacierettes for your catchment area.

2. Delineate individual watersheds (as outlined in Appendix C) for each glaciated catchment. If glacier shapefiles straddle multiple catchments, then clip them into their respective watershed boundaries.

3. Clip the DEM into individual watersheds using the "Spatial Analyst" (Mask) and "Raster Calculator" tools

4. Export the clipped DEMs into Excel and sort the elevation data by your specified 2 – 16 elevation zones. Generate a weighted hypsometric mean for each elevation zone. These data will be your hypsometric mean inputs into SRM.

5. Using the "Reclassify" tool, reclassify each DEM into your 2 – 16 zones.

6. Using the "Merge" feature, combine all glaciers, snowfields, and glacier segments that are within a common watershed. Do this for each watershed.

7. Clip the reclassed watershed DEMs to the combined glacier coverage shapefiles, using the "Spatial Analyst" (Mask) and "Raster Calculator" tools.

8. Repeat step 7 for the debris-covered glacier shapefiles.

9. From their respective attribute tables, export the area values for glacier coverage, debris-covered glaciers, and total area within each zone into Excel. Do this for each watershed.

10. In Excel, calculate the fraction of glaciation for each elevation zone and watershed. Both the fraction of glaciation and area of each elevation zone are required SRM inputs.

Appendix D. The degree day factors applied to the SRM calibration, validation, and 2007 simulations.

zone #	DDF (mm $^{o}C^{-1}$ d^{-1})	Elevation Range (m)	Hypsometric Mean Elevation (m)	Total Area (km^2)	Glacier Area (km^2)	Glacier Fraction
Eliot Glacier Catchment						
1	0.06	1800-2000	1944	0.279	0.145	0.519
2	0.38	2001-2200	2092	0.600	0.392	0.652
3	0.61	2201-2400	2311	0.703	0.459	0.653
4	0.44	2401-2600	2496	0.549	0.357	0.651
5	0.44	2601-2800	2698	0.393	0.321	0.817
6	0.44	2801-3000	2878	0.203	0.111	0.544
7	0.44	3001-3200	3097	0.110	0.045	0.410
8	0.44	3201-3400	3303	0.112	0.012	0.105
Coe Glacier Catchment						
1	1.2	1778-2000	1906	0.294	0.144	0.489
2	5.0	2001-2200	2093	0.416	0.167	0.400
3	4.3	2201-2400	2306	0.518	0.235	0.453
4	4.4	2401-2600	2494	0.431	0.340	0.789
5	4.4	2601-2800	2699	0.281	0.117	0.417
6	4.4	2801-3000	2889	0.194	0.140	0.726
7	4.4	3001-3200	3086	0.096	0.083	0.860
8	4.4	3201-3400	3234	0.010	0.007	0.727
Compass Catchment						
1	7.1	1572-2000	1827	1.229	0.002	0.001
2	7.1	2001-2200	2094	0.625	0.068	0.110
3	4.8	2201-2400	2292	0.374	0.119	0.317
4	4.4	2401-2600	2483	0.163	0.056	0.343
5	4.4	2601-2800	2671	0.024	0.024	1.000

Appendix E. SRM Calibration Parameters for the Eliot Glacier Discharge, 8/1/07 – 9/29/07. Constants: Recession Y-coefficient – 0.1, Rainfall Runoff Coefficient – 0.7

Date	Actual Q	Temp °C max	Temp °C min	Precip (cm)	Snow Runoff Coefficient	Recession x-coeffient	Comp Q
8/1/07	0.733	25	12.2	0	0.7	0.25	0.832
8/2/07	0.762	23.9	12.2	0	0.7	0.25	0.837
8/3/07	0.669	18.9	8.9	0.3	0.7	0.25	0.74
8/4/07	0.521	19.4	6.7	0	0.7	0.25	0.596
8/5/07	0.431	19.4	7.8	0	0.7	0.25	0.539
8/6/07	0.472	16.7	6.7	0	0.7	0.25	0.477
8/7/07	0.56	16.1	3.9	0	0.85	0.25	0.405
8/8/07	0.724	16.7	6.7	0	0.85	0.25	0.439
8/9/07	0.578	15.6	6.1	0	0.85	0.25	0.453
8/10/07	0.507	15.6	4.4	0	0.85	0.25	0.405
8/11/07	0.463	18.9	6.7	0	0.85	0.25	0.48
8/12/07	0.439	16.1	8.3	0	0.85	0.25	0.539
8/13/07	0.509	20	9.4	0	0.85	0.25	0.634
8/14/07	0.728	23.3	11.1	0	0.85	0.25	0.809
8/15/07	0.907	24.4	13.3	0	0.85	0.25	0.97
8/16/07	0.833	14.4	8.3	0.3	0.85	0.25	0.796
8/17/07	0.49	12.8	7.2	0	0.85	0.25	0.517
8/18/07	0.319	11.1	3.9	0.3	0.85	0.25	0.334
8/19/07	0.491	12	4.4	2.12	0.85	0.25	0.456
8/20/07	0.565	12	6	3.02	0.85	0.25	0.726
8/21/07	0.497	12	4.4	0	0.85	0.25	0.537
8/22/07	0.458	15	8.3	0	0.85	0.25	0.442
8/23/07	0.486	20	7.8	0	0.85	0.25	0.602
8/24/07	0.521	21.7	9.4	0	0.85	0.25	0.764
8/25/07	0.591	17.2	8.9	0	0.85	0.25	0.726
8/26/07	0.41	11.7	3.3	0	0.85	0.25	0.431
8/27/07	0.395	15.6	2.8	0	0.85	0.25	0.297
8/28/07	0.436	18.3	6.1	0	0.85	0.25	0.418
8/29/07	0.692	23.9	10.6	0	0.85	0.25	0.717
8/30/07	0.92	24.4	15	0	0.85	0.25	0.999
8/31/07	0.97	17.8	11.7	0	0.85	0.25	0.917
9/1/07	0.758	18.9	6.7	0	0.85	0.25	0.704
9/2/07	0.599	17.8	10.6	0	0.85	0.25	0.667
9/3/07	0.582	19.4	11.1	0	0.85	0.1	0.742
9/4/07	0.609	12.2	6.1	0	0.95	0.1	0.524
9/5/07	0.51	17.2	4.4	0	0.95	0.1	0.434
9/6/07	0.432	14.4	5	0	0.95	0.1	0.42
9/7/07	0.29	15.6	6.1	0	0.45	0.1	0.299
9/8/07	0.207	13.9	7.2	0	0.45	0.1	0.229
9/9/07	0.17	14.4	8.9	0	0.45	0.1	0.243

Appendix E. (Continued)

9/10/07	0.251	18.9	10.6	0	0.4	0.1	0.309
9/11/07	0.378	23.9	12.2	0	0.4	0.1	0.414
9/12/07	0.392	21.1	11.1	0	0.4	0.1	0.425
9/13/07	0.373	17.8	10.6	0.3	0.4	0.1	0.412
9/14/07	0.299	17.2	4.4	0	0.4	0.1	0.295
9/15/07	0.213	16.1	3.9	0	0.4	0.1	0.194
9/16/07	0.193	11.7	5.6	0.91	0.4	0.1	0.252
9/17/07	0.16	8.9	2.8	0.91	0.4	0.1	0.197
9/18/07	0.075	7.8	-1.7	0.3	0.4	0.1	0.061
9/19/07	0.024	8.3	-1.1	0.3	0.4	0.1	0.011
9/20/07	0.064	12.8	2.2	0	0.4	0.1	0.03
9/21/07	0.082	16.7	2.2	0	0.4	0.1	0.058
9/22/07	0.052	10.6	0	0	0.4	0.1	0.04
9/23/07	0.025	6.7	-1.7	0	0.4	0.1	0.011
9/24/07	0.026	10.6	-1.1	0	0.4	0.1	0.008
9/25/07	0.031	12.8	2.8	0	0.4	0.1	0.03
9/26/07	0.046	17.8	5.6	0	0.4	0.1	0.069
9/27/07	0.077	16.1	6.7	0	0.4	0.1	0.087
9/28/07	0.02	6.1	-1.7	2.12	0.4	0.1	0.039
9/29/07	0.02	2.2	-3.3	4.84	0.4	0.1	0.005

Appendix F. Measured ^{18}O Compositions in the Coe and Eliot Watersheds.

Spring-fed Inputs

9/10/2007	14:10	Coe Spring	-11.63
9/13/2007	14:06	Eliot Spring 1	-11.53
9/13/2007	14:40	Eliot Spring 2	-11.63
		Average	**-11.60**

Lower Eliot Surface Water

8/24/2007	17:12	Lower Eliot	-13.02
9/14/2007	7:27	Lower Eliot	-13.26
10/13/2007	21:57	Lower Eliot	-13.59
		Average	**-13.29**

Eliot Glacier Meltwater

8/24/2007	16:06	Upper Eliot	-13.22
9/14/2007	8:47	Upper Eliot	-13.74
10/13/2007	19:00	Upper Eliot	-14.23
		Average	**-13.73**

Eliot Glacier Ice

8/24/2007	16:00	Eliot Ice (near probe)	-15.42
9/15/2007	12:40	Eliot Glacier Crevasse 1	-15.64
10/13/2007	16:10	Eliot Ice (near probe)	-14.29
10/13/2007	17:58	Upper Rock Glacier Ice	-13.98
		Average	**-14.83**

Eliot Snow

10/13/2007	17:02	Lower Rock Glacier Snow	-10.98
10/13/2007	17:34	Upper Rock Glacier Snow	-10.36
10/7/2007	14:20	Snow on Trail between Eliot and Coe	-9.96
		Average	**-10.43**

Lower Coe Surface Water

8/24/2007	13:30	Lower Coe	-12.67
9/11/2007	22:10	Lower Coe	-12.40
		Average	**-12.54**

Coe Glacier Meltwater

8/24/2007	13:30	Upper Coe	-12.82
9/11/2007	16:40	Upper Coe	-12.74
		Average	**-12.78**

Coe Glacier Ice

8/24/2007	13:30	Coe Ice	-13.52
9/11/2007	13:20	Coe Ice	-13.19
		Average	**-13.36**